

# High Pressure Applications

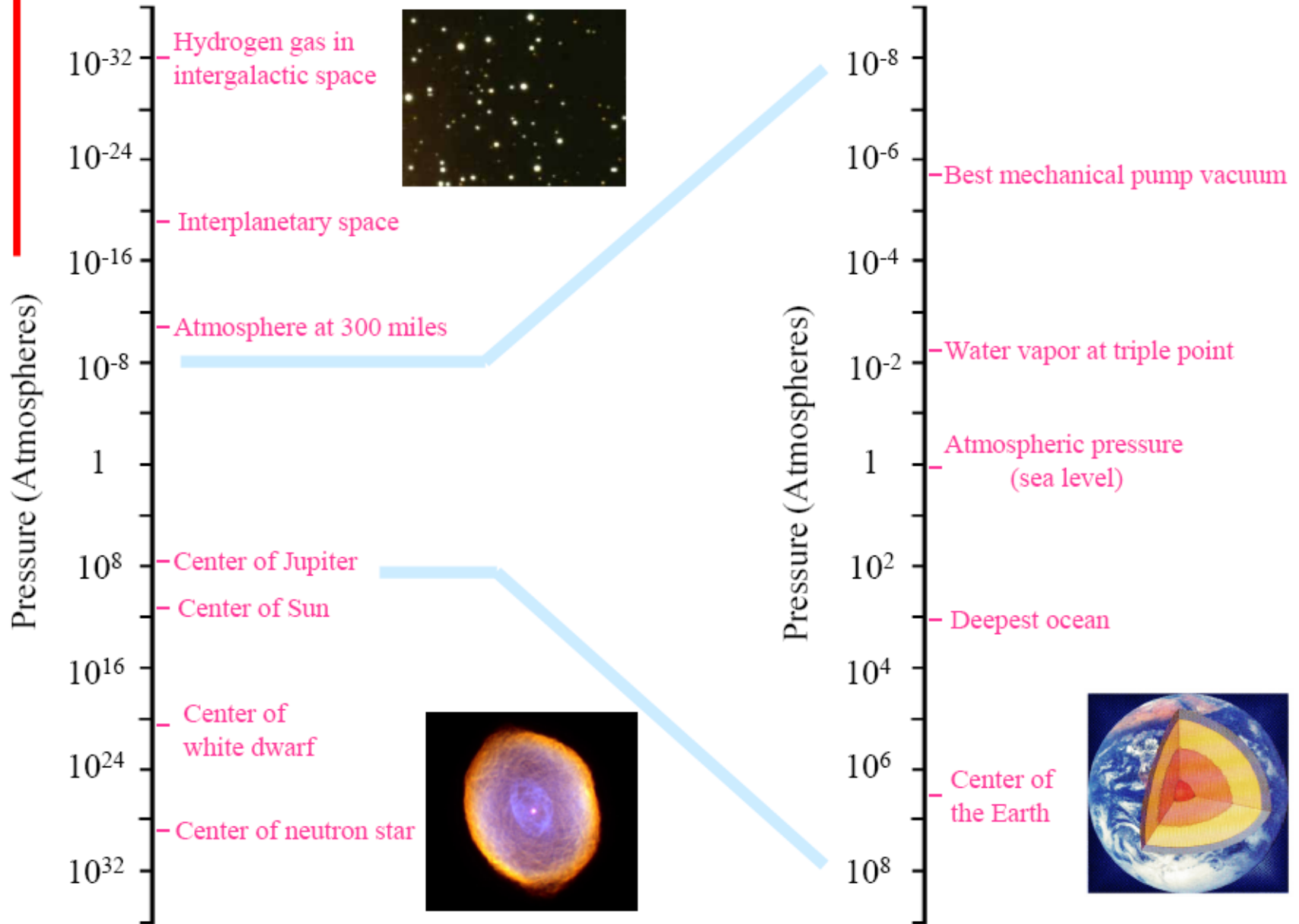
Haozhe Liu

HPSTAR, Changchun/Beijing, China

# Outline

- High pressure techniques (brief history)
- Pressure calibration
- Equation of state (EoS)
- Cases using synchrotron techniques

# RANGE OF PRESSURE IN THE UNIVERSE



# Unit

- Pressure: Force & Area

$$P=F/A$$

- SI unit: Pascal (Pa)
- One bar = 100,000 Pa=750.062 torr = 0.9869 atm
- 1 atmosphere pressure (sea level)
- 1 atm = 760 torr = 14.7 psi
- **Popular:**

**GPa = 9,870 atm = 10,000 bar.**

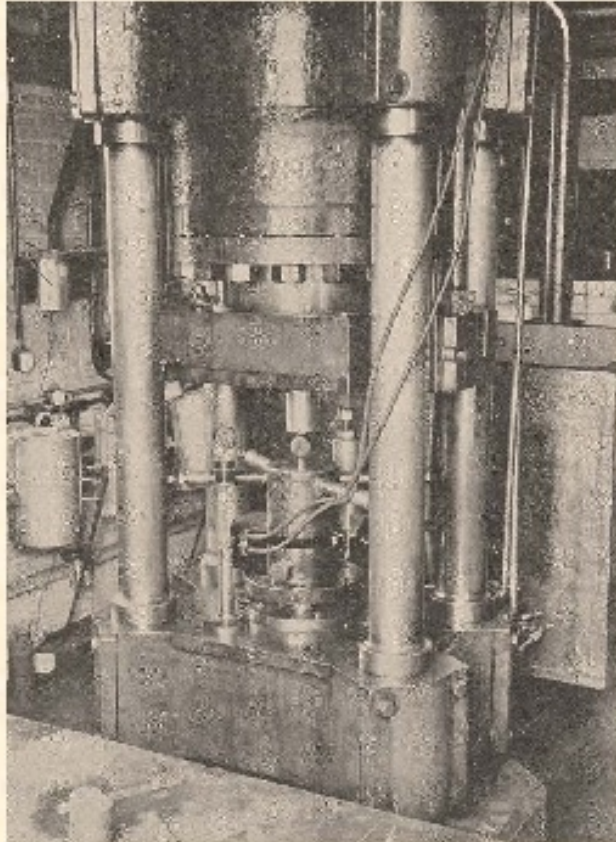
**Kbar**

# High Pressure Technology

- Dynamic HP  
Shock Wave and Detonation

- Static HP
  1. Large volume press
  2. Small volume cell  
DAC (Diamond Anvil Cell)

# High-Pressure Technology: CHALLENGES AND BIRTH OF THE FIELD



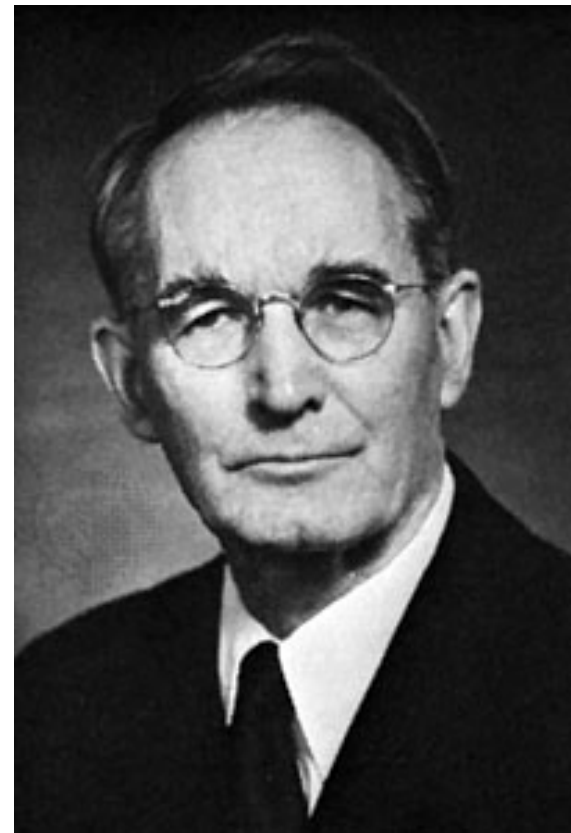
**“The difficulties of making exact measurements of any physical quantity whatever under the conditions outlined are very considerable and much time is consumed merely devising tools for the enterprise.”**

**E. D. Williamson, “Change of the Physical Properties of Materials with Pressure,” *J. Franklin Inst.* 193, 491 (1922).**

# Percy Williams Bridgman

(1882-1961)

- Bridgman published more than 260 papers (only two of which listed a coauthor) and 13 books.
- His scientific papers have been published in *Collected Experimental Papers*, 7 vol. (1964).
- Among his many books are *The Physics of High Pressure* (1931) and *Reflections of a Physicist* (1950).



# Nobel Lecture, December 11, 1946

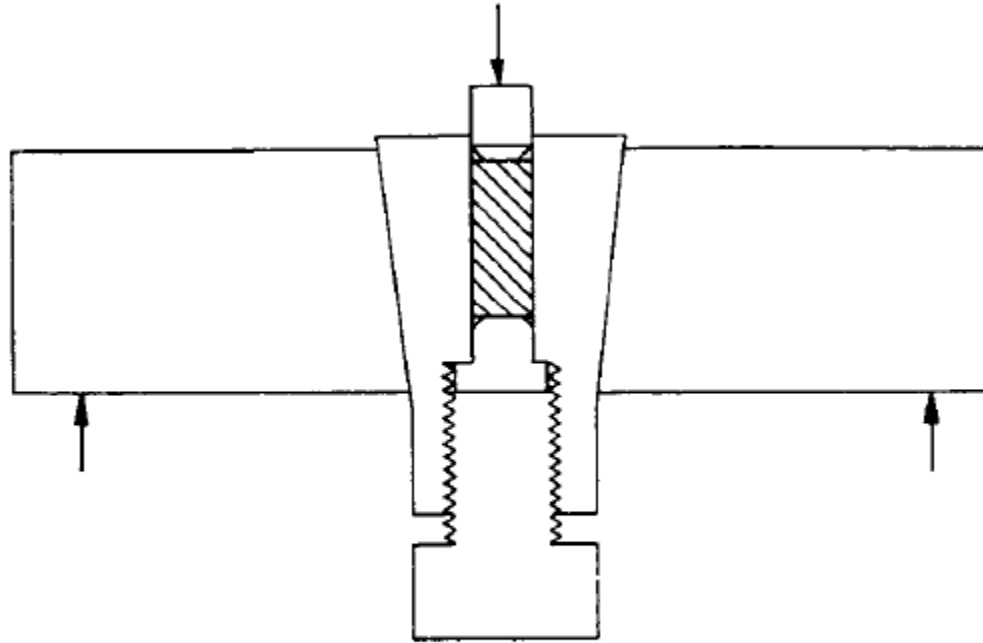


Fig. 2. Illustrating the general principle of the method for giving external support to the pressure vessel in such a way that support increases automatically with the increase of internal pressure.

Strength of materials!

# Polymorphism

## Compressibility

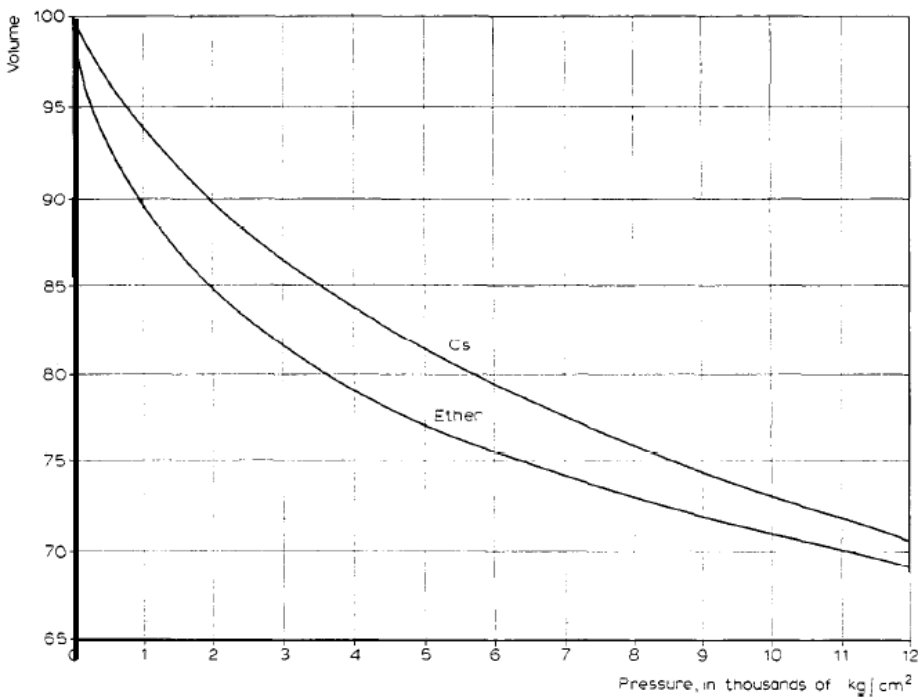


Fig. 5. Volume as a function of pressure for a typical liquid, ether. The corresponding curve is also shown for caesium, the most compressible solid. The liquid is initially much more compressible than the solid, but at higher pressures is less compressible.

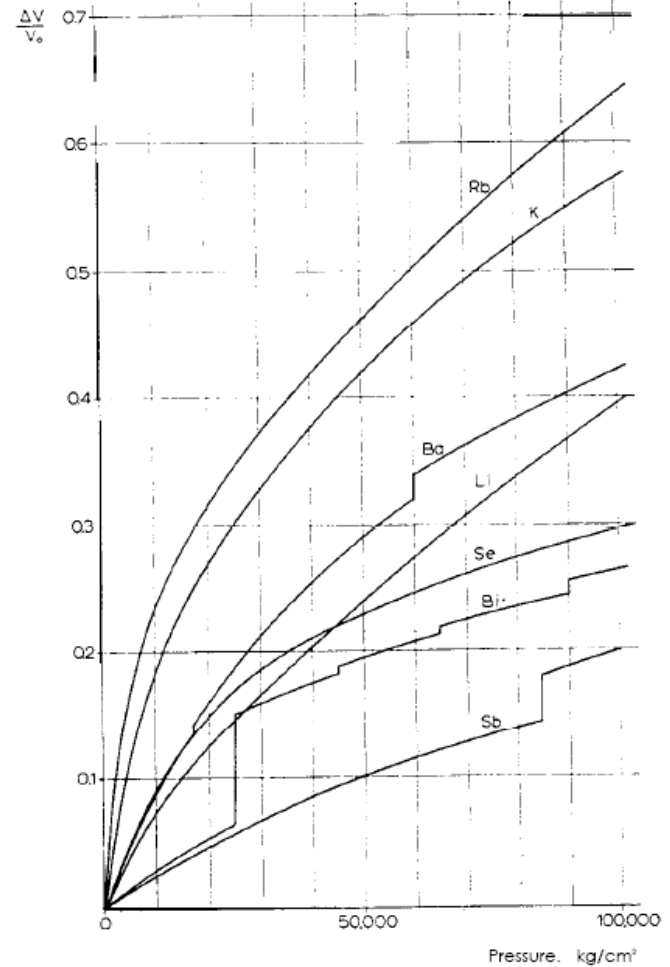


fig. 6. The volume compression of several elements up to 100,000 kg/cm². The breaks in some of the curves indicate polymorphic transitions.

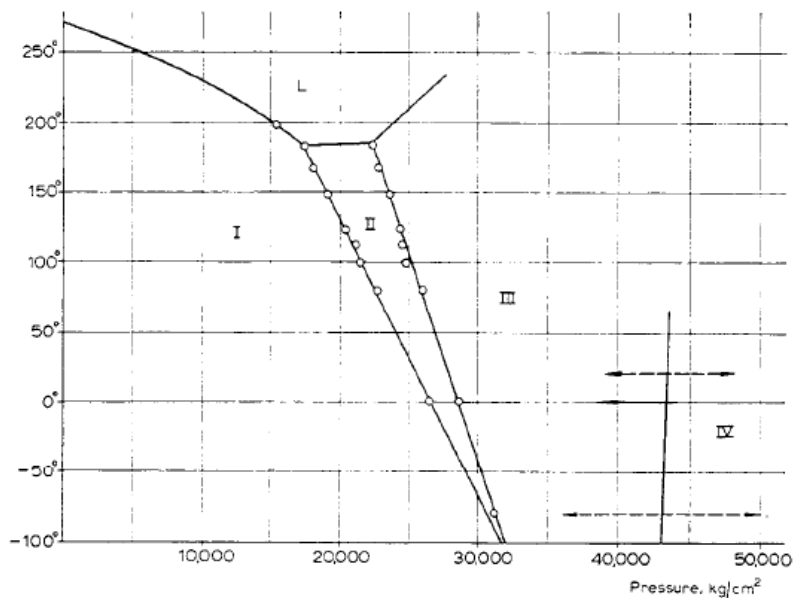


Fig. 9. The phase diagram of bismuth. The arrows on the transition line III-IV indicate the pressure limits within which the transition runs with increasing or decreasing pressure.

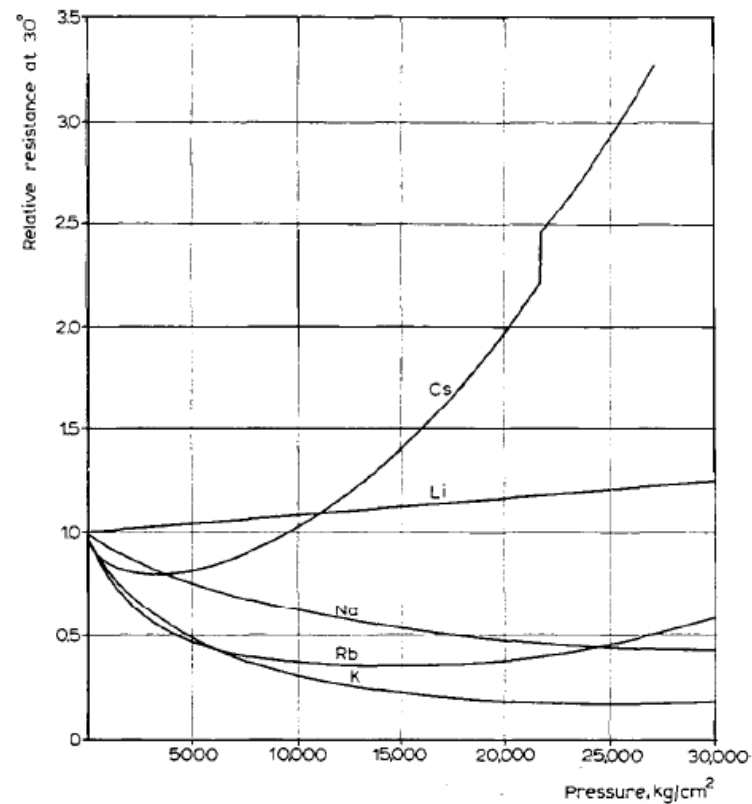
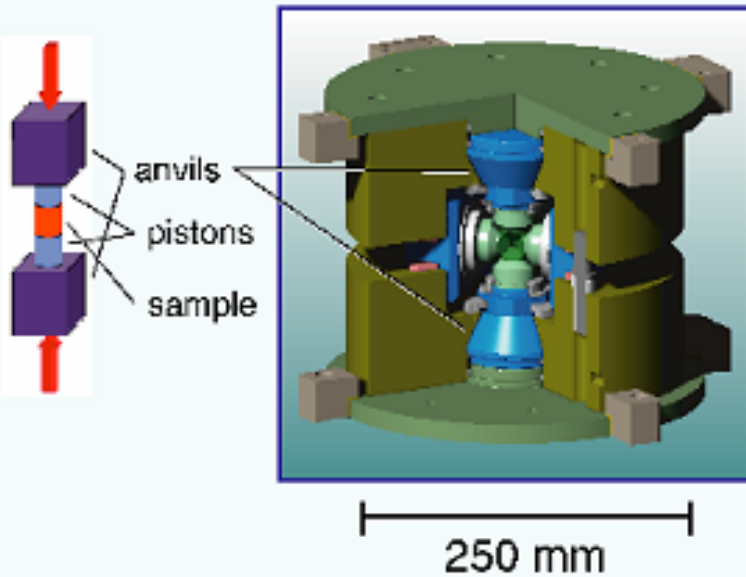


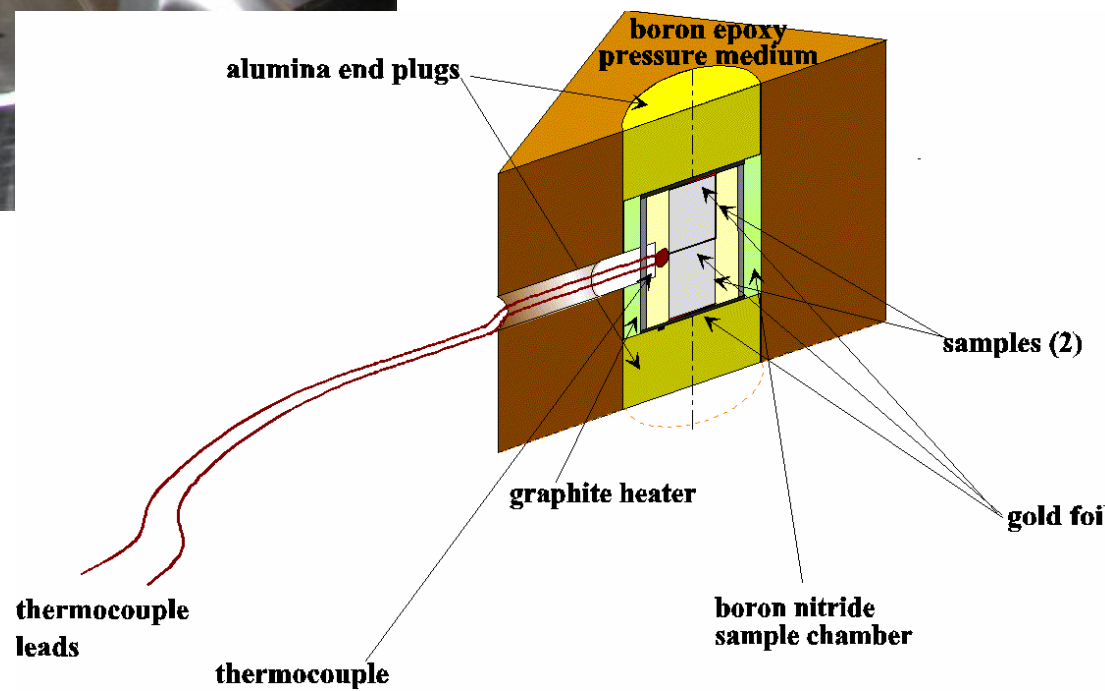
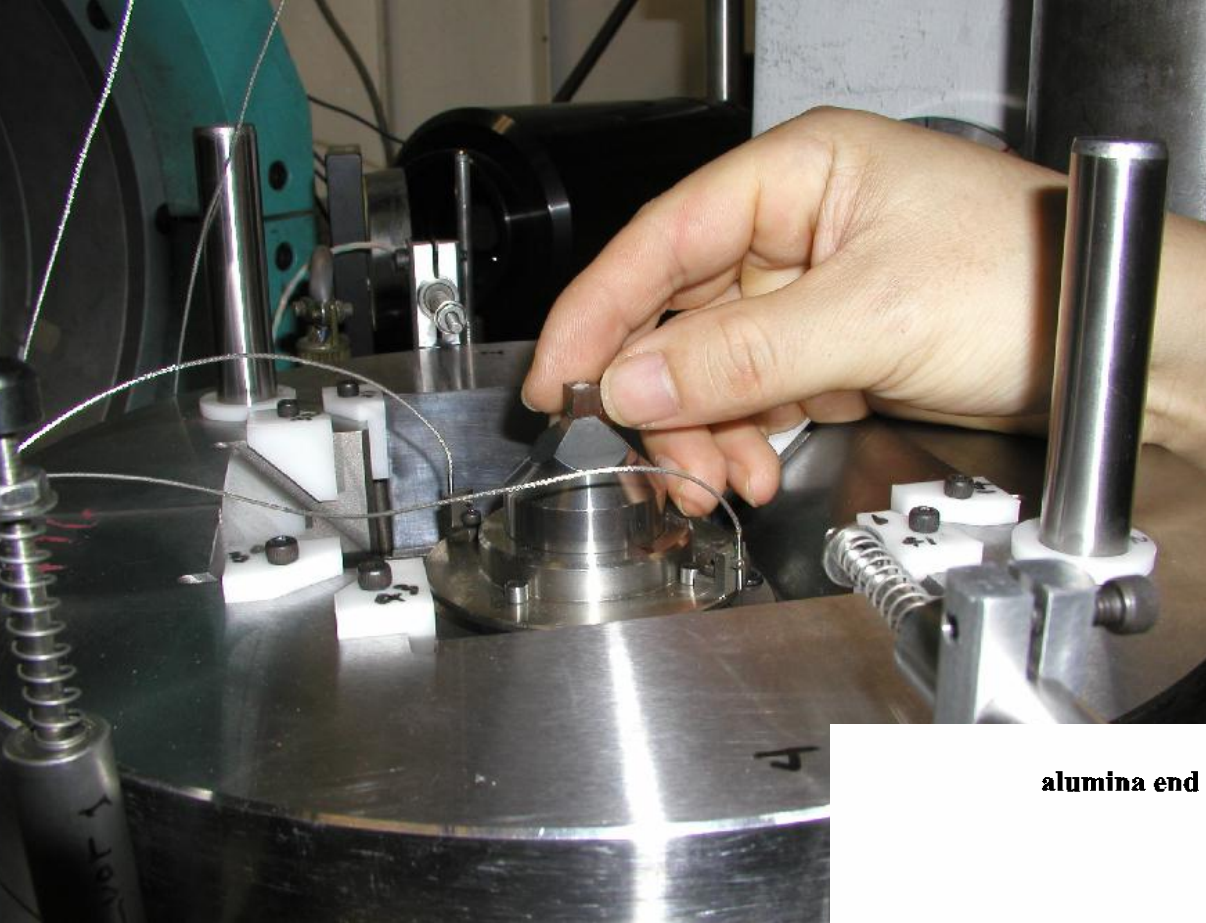
Fig. 10. The relative resistances of the alkali metals up to 30,000 kg/cm². The break in the curve for caesium is due to a polymorphic transition. Potassium has a very flat minimum near 23,000.

# Large Volume Press (LVP)

Deformation-DIA (D-DIA)



*Novatek Cubic Press*



# HP Applications

## Syntheses *via* Pressure

- Superhard materials

Diamond , c-BN,

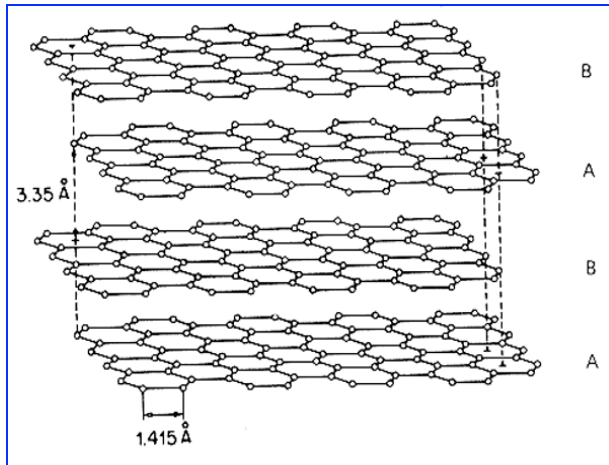
- Superconductor:



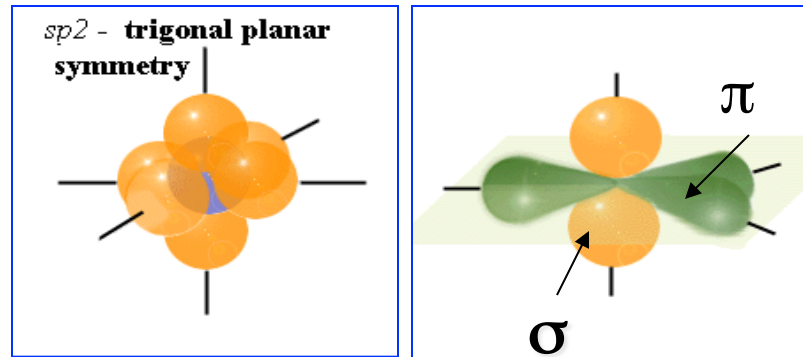
- Super “hot” materials:



# GRAPHITE

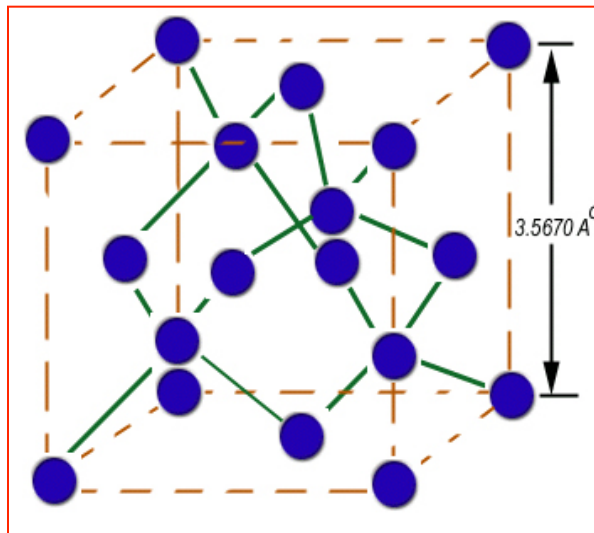


# *sp*<sup>2</sup> carbon bonding

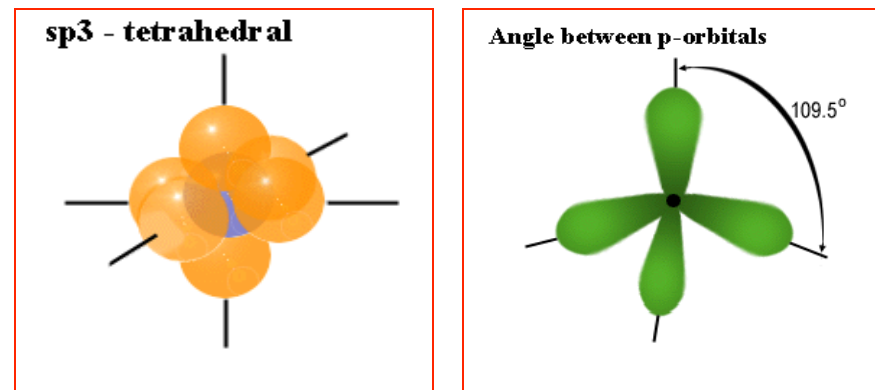


*sp*<sup>2</sup> has 3 coplanar (strong) sigma-bonds & 2 (weak) p-bonds with 360° influence

# DIAMOND



# *sp*<sup>3</sup> – carbon bonding



*sp*<sup>3</sup> has 4 “sigma” (strong) bonds

# High Pressure Man-made Diamond

December 16, 1954, Tracy Hall  
*et al* of General Electric

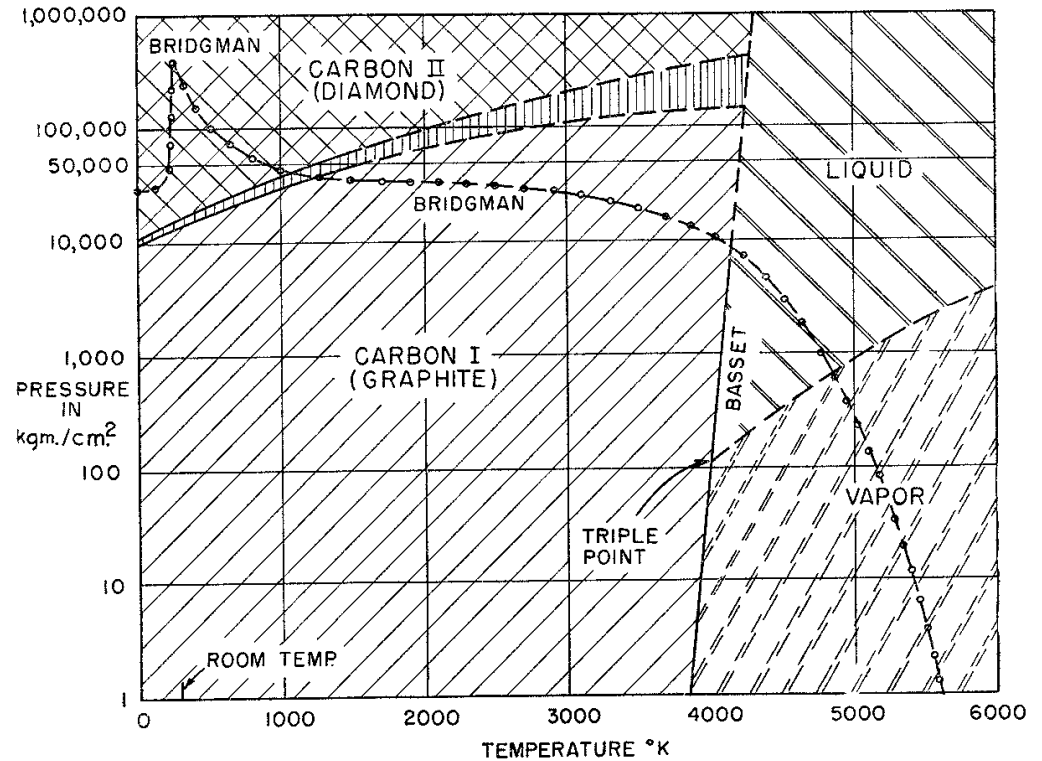
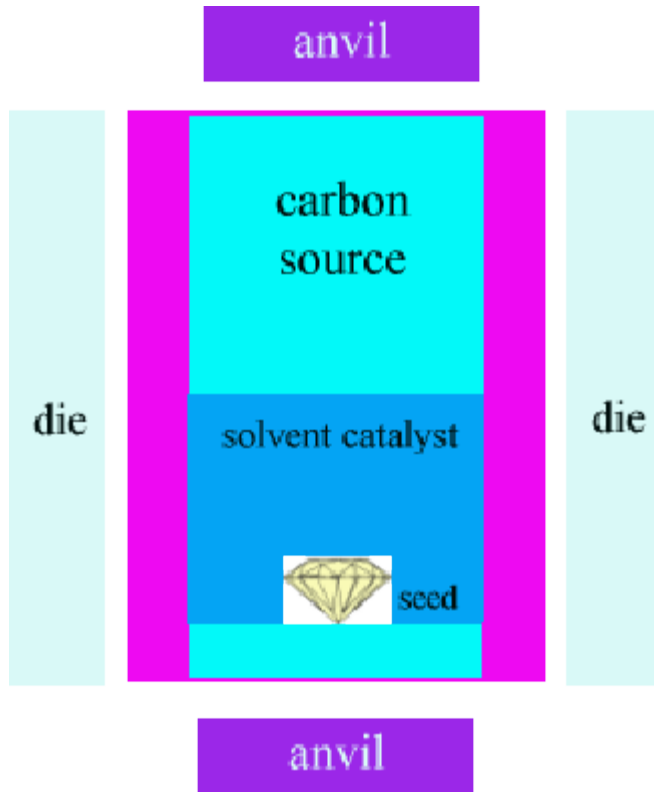
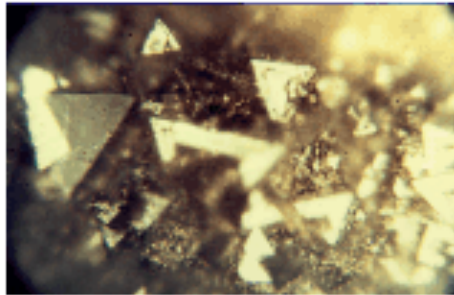


Fig. 1. Phase diagram of carbon

F.P Bundy, H.T. Hall, H.M. Strong, R.H. Wentorf, *Nature*, **176**, 51 (1955)

On December 16, 1954, his work paid off. Dr. Hall opened the capsule from his "belt" and saw the triangular facets of what he immediately recognized to be man-made diamonds.



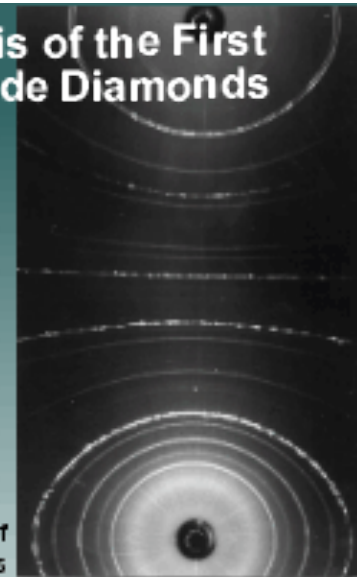
Dr. Hall's First Man-made Diamond Crystals

*"My hands began to tremble, my heart beat rapidly, my knees weakened, and no longer gave support."*

Dr. Hall and others repeated his experiment successfully and G.E. made its announcement to the world, Feb. 15, 1955.

X-Ray Diffraction Pattern (fingerprint) of Dr. Hall's Man-made Diamonds

## Synthesis of the First Man-made Diamonds



THE PROBLEMS

High Temperature/High Pressure "Belt" Apparatus

Experimental Stages

NEXT ▲

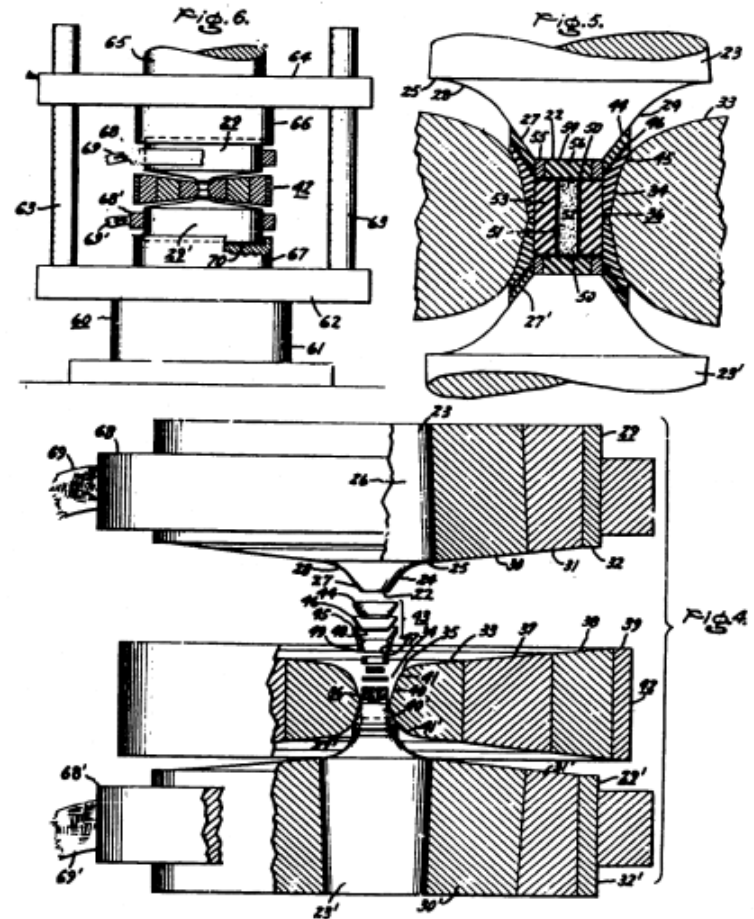


Dr. H. Tracy Hall with first man-made diamonds

## High Temperature/High Pressure Belt Apparatus

In the Fall of 1954, Dr. Hall completed development of the "the Belt" apparatus. (U.S. Patent Number 2,941,248)

This apparatus allowed scientists to reach pressures of 75,000 atmospheres (1 million psi) with simultaneous temperatures of over 2,000 C.



THE PROBLEMS

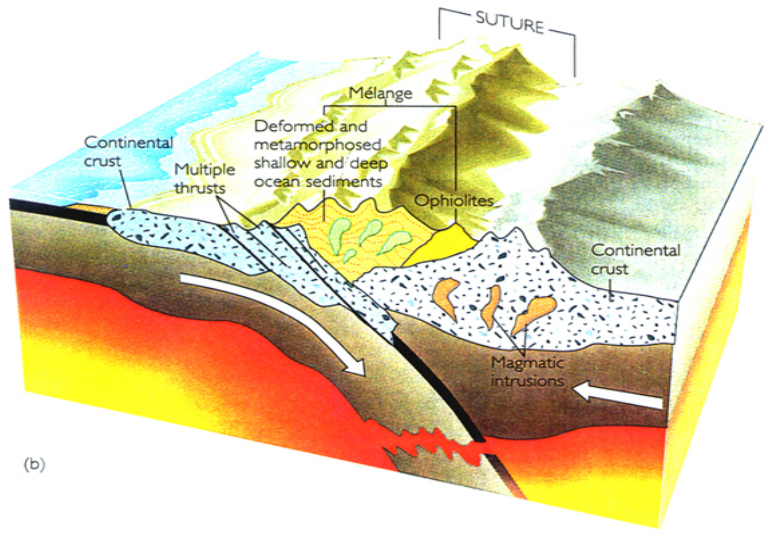
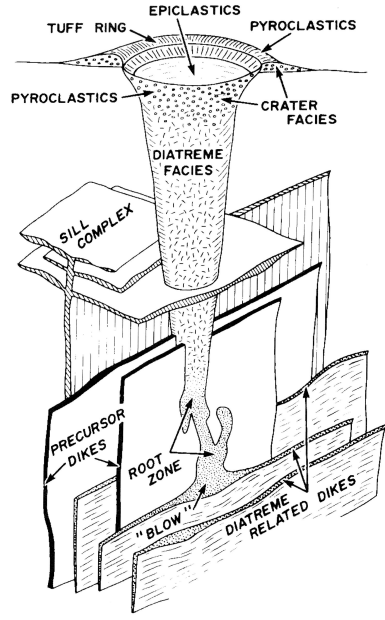
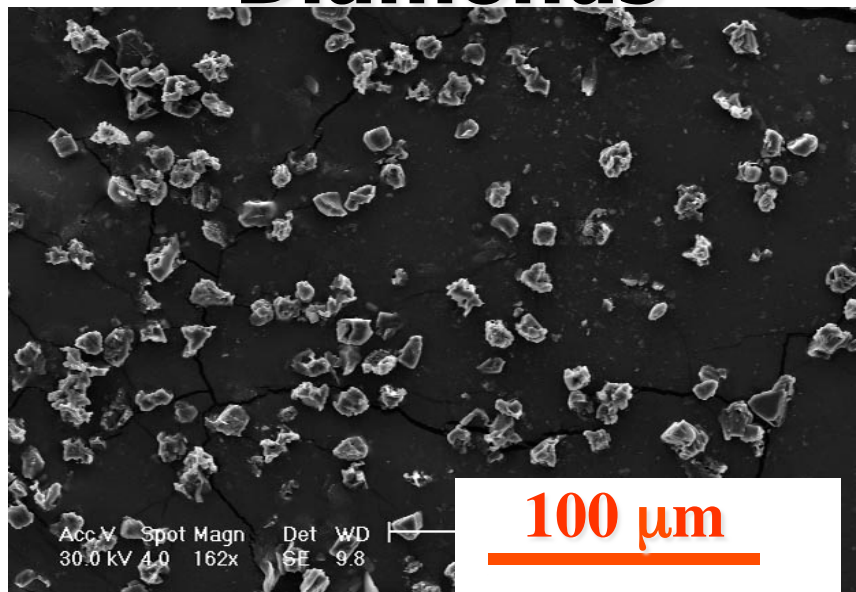
Experimental Stages

Inventor:  
 Howard Tracy Hall,  
 by Paul G. Franke  
 His Attorney.

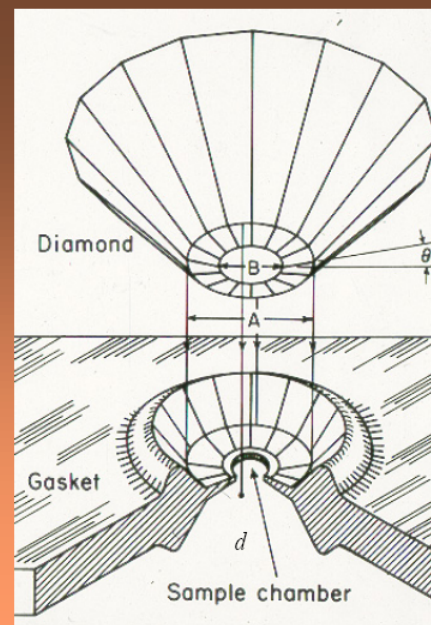
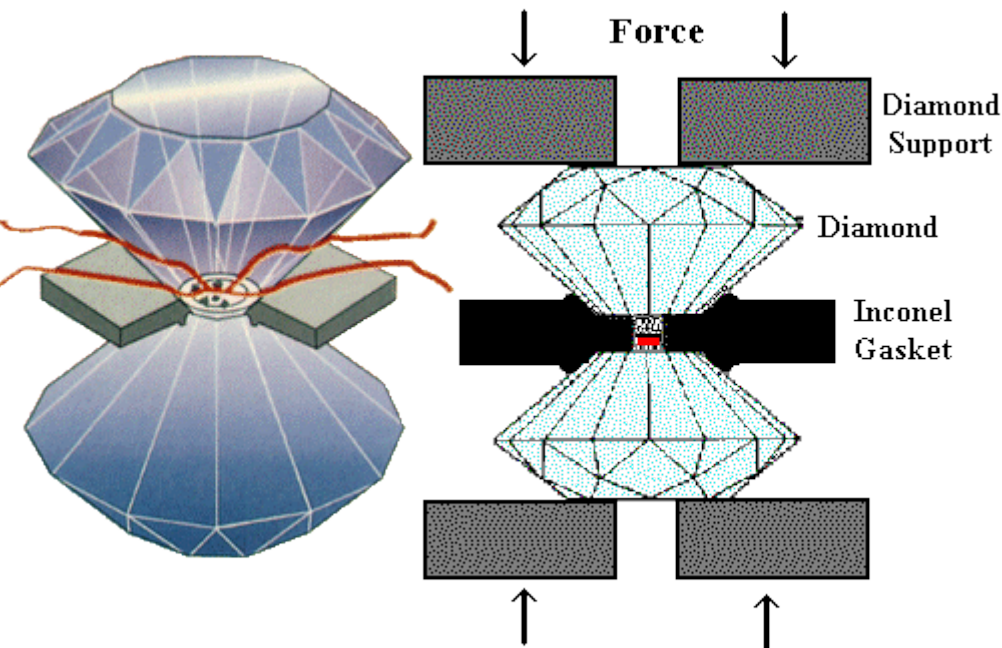
# Kimberlitic Diamond



# Subduction Zone Diamonds



# Diamond anvil cell (DAC)



## CONVENTIONAL MEGABAR DIAMOND ANVIL CELL



<i>P</i>	<i>d</i>	<i>Volume</i>
50 GPa	~200 $\mu\text{m}$	~10 nl ( $10^{-9}$ l)
200 GPa	~20 $\mu\text{m}$	~1 pl ( $10^{-12}$ l)

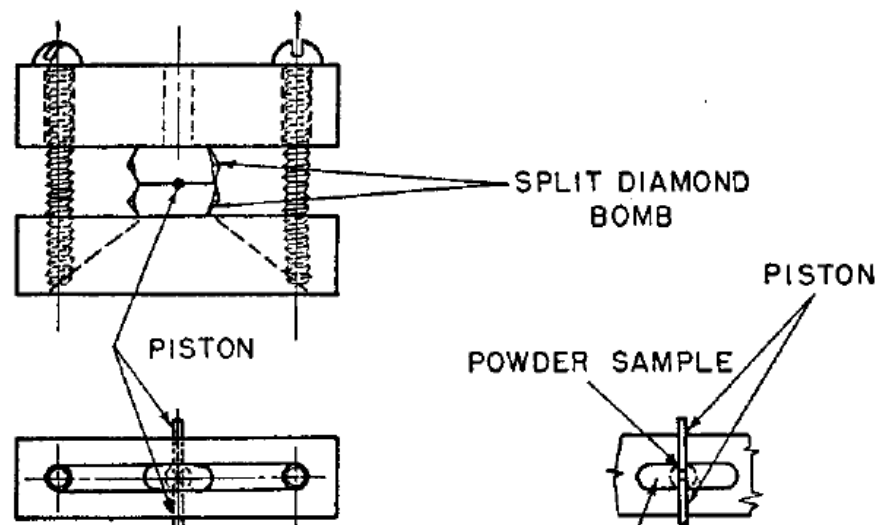
# A Diamond Bomb for Obtaining Powder Pictures at High Pressures

A. W. LAWSON AND TING-YUAN TANG

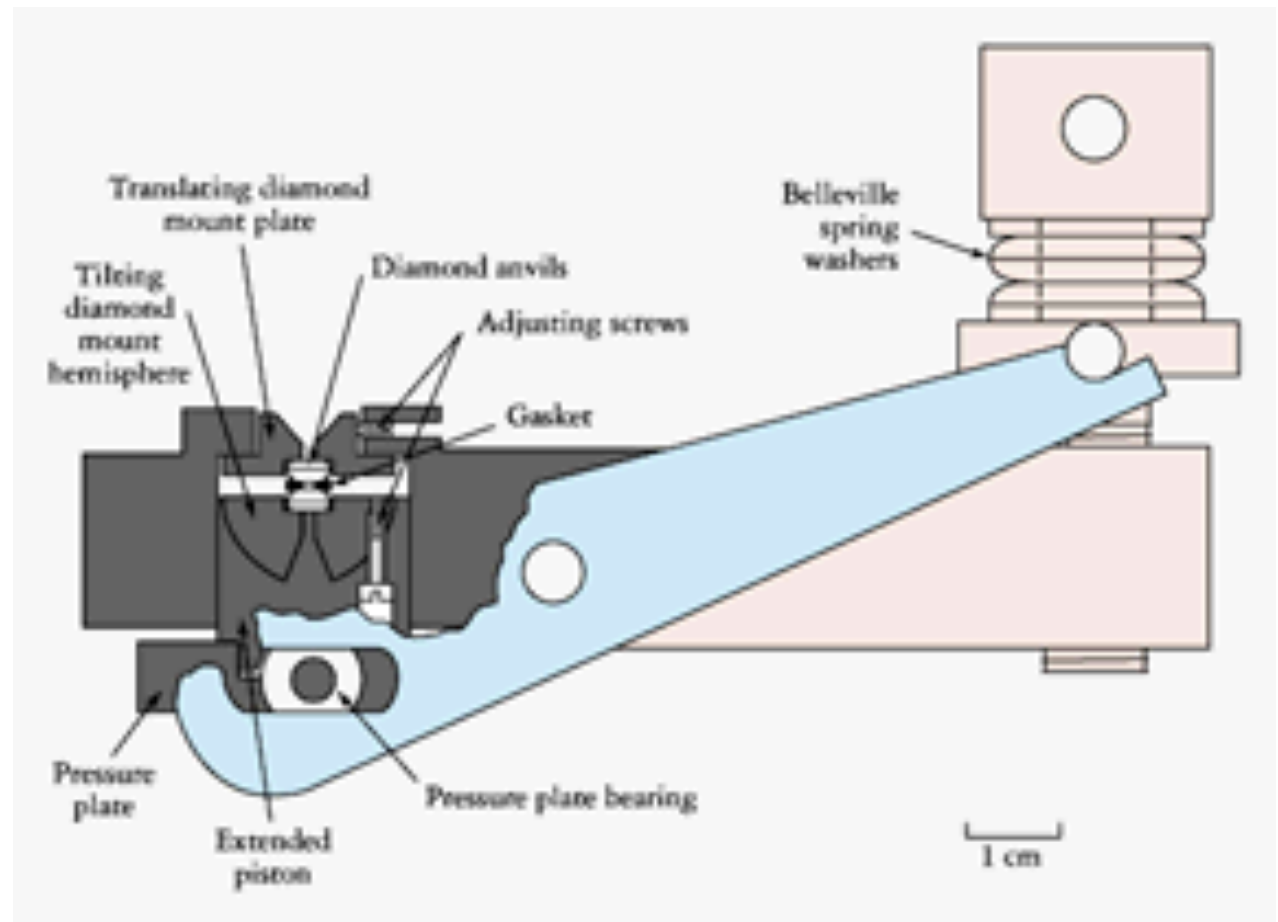
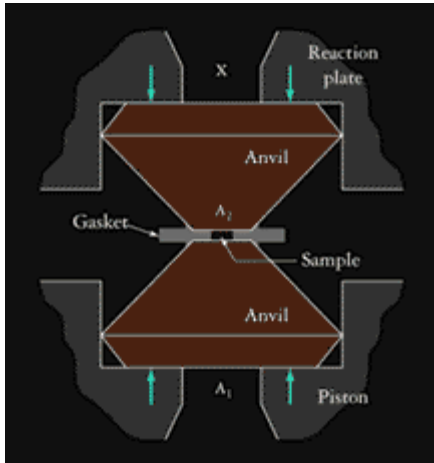
*Institute for the Study of Metals, University of Chicago, Chicago, Illinois*

July 7, 1950

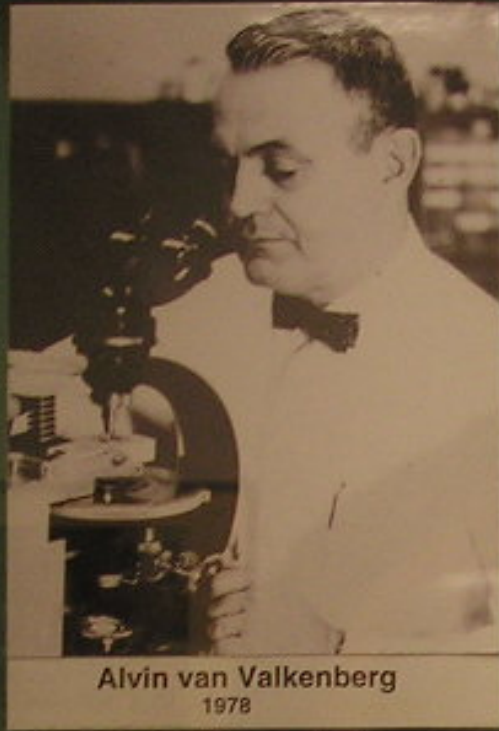
RECENTLY a procedure for obtaining x-ray powder diffraction patterns of materials subjected to high hydrostatic pressures has been described in this journal by N. A. Riley and one of the authors.<sup>1</sup> This technique involves the use of a large grain size beryllium bomb for retaining the pressure. Transmission diffraction patterns of samples retained by the bomb are obtained by traversing both the bomb and the sample with an x-ray beam



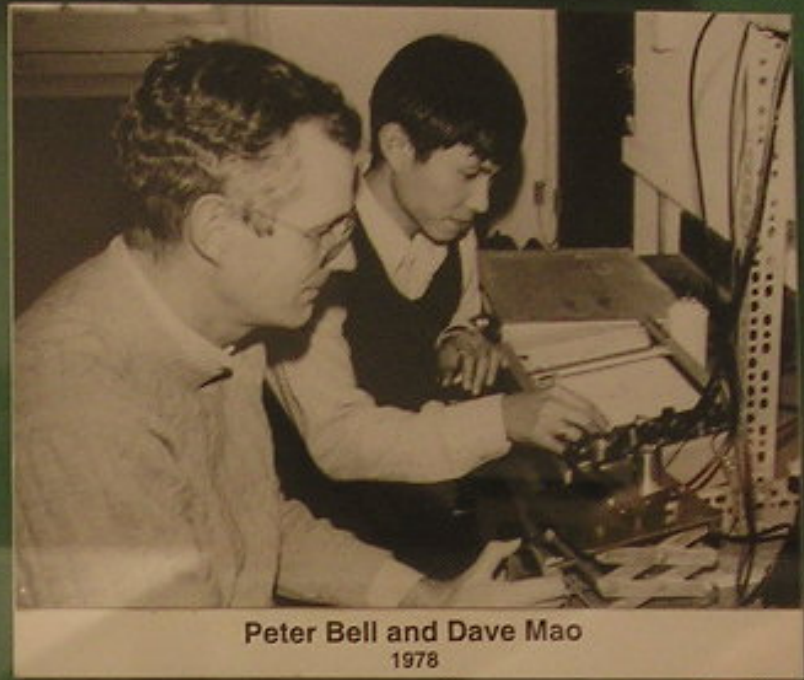
The lever-arm diamond anvil cell, as diagrammed here: by the application of leverage a turn of a screw could create many thousands of atmospheres of pressure



- C. E. Weir, E. R. Lippincott, A. Van Valkenburg, and E. N. Bunting, Infrared Studies in the 1-to 15-Micron Region to 30,000 Atmospheres, *J. Res. Natl. Bur. Stand.* **63A**, 55-62 (1959).
- Alvin Van Valkenburg, Visual Observations of High Pressure Transitions, *Rev. Sci. Instrum.* **33**, 1462 (1962).



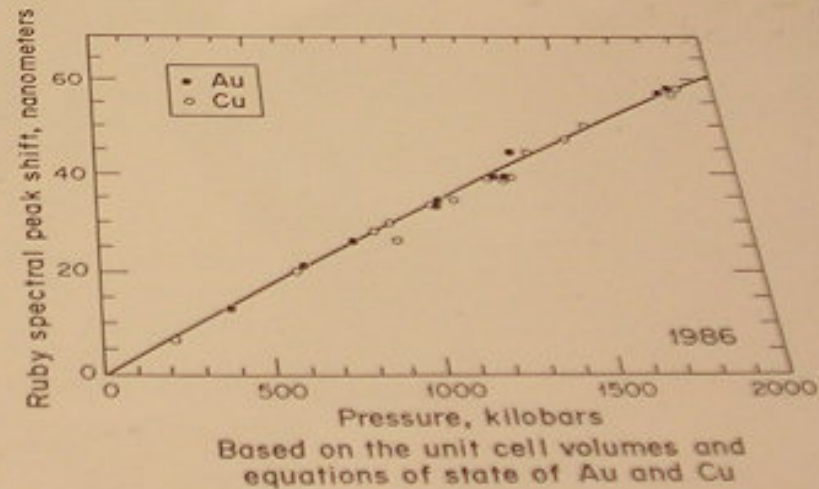
Alvin van Valkenberg  
1978



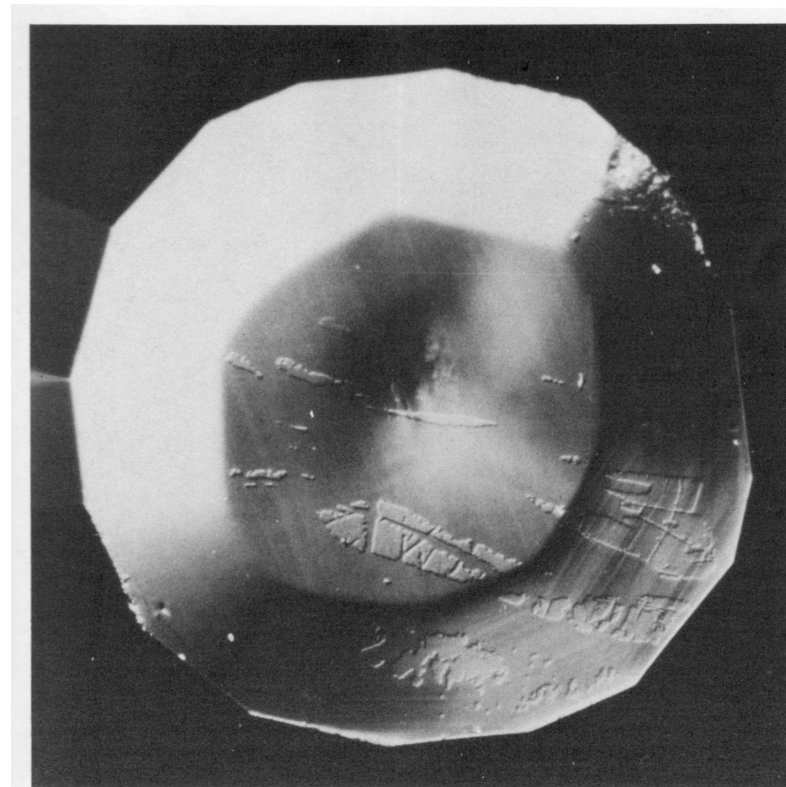
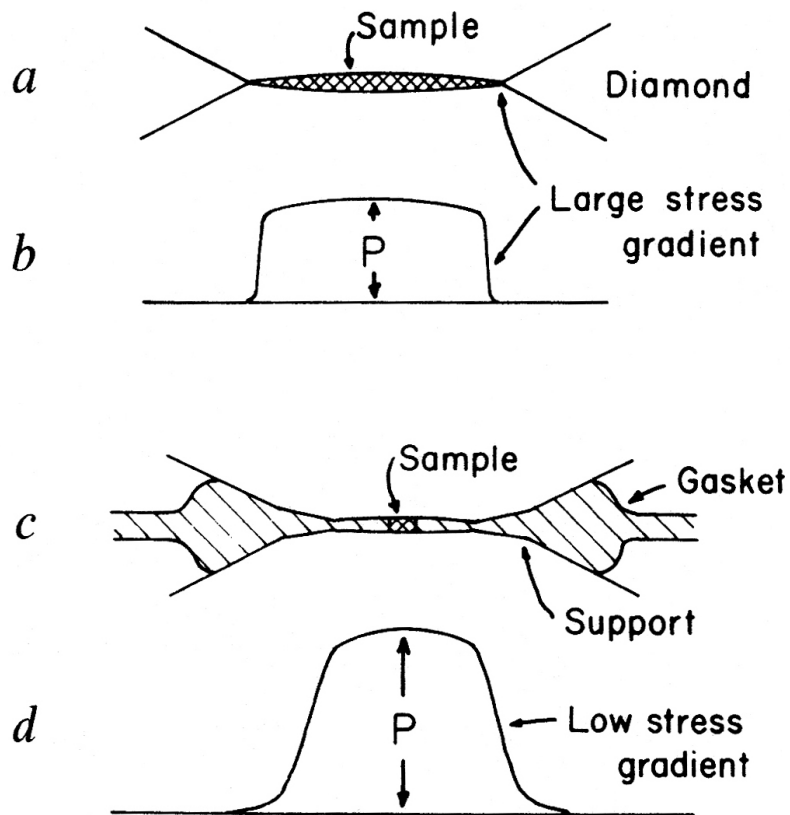
Peter Bell and Dave Mao  
1978

Alvin Van Valkenburg, pictured here in 1963, was a pioneer in using the diamond anvil cell to study materials at high pressure at the National Bureau of Standards (NBS), Washington DC.

now the National Institute of Standards and Technology (NIST)



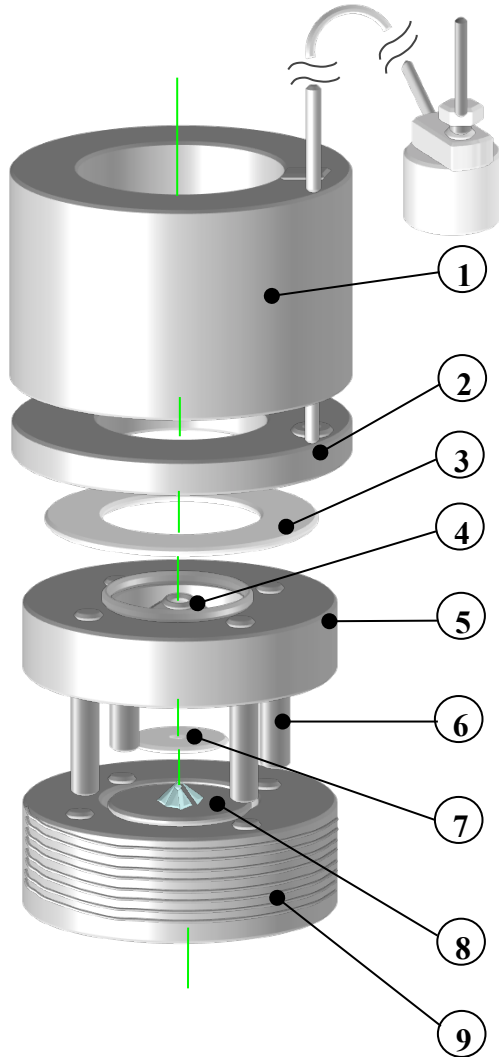
PRESSURE CALIBRATION



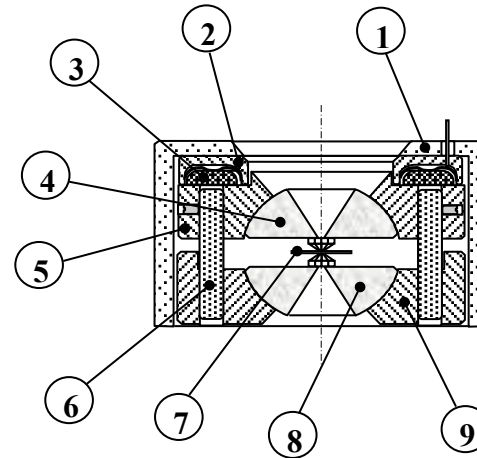
Distorted anvil face due to plastic deformation at 1.7 Mbar  
Mao and Bell, 1978

Anvil distortion and effect on pressure distribution  
a,b unbeveled anvils, c,d beveled anvils  
Mao and Bell, 1978

# Gas driven membrane DAC

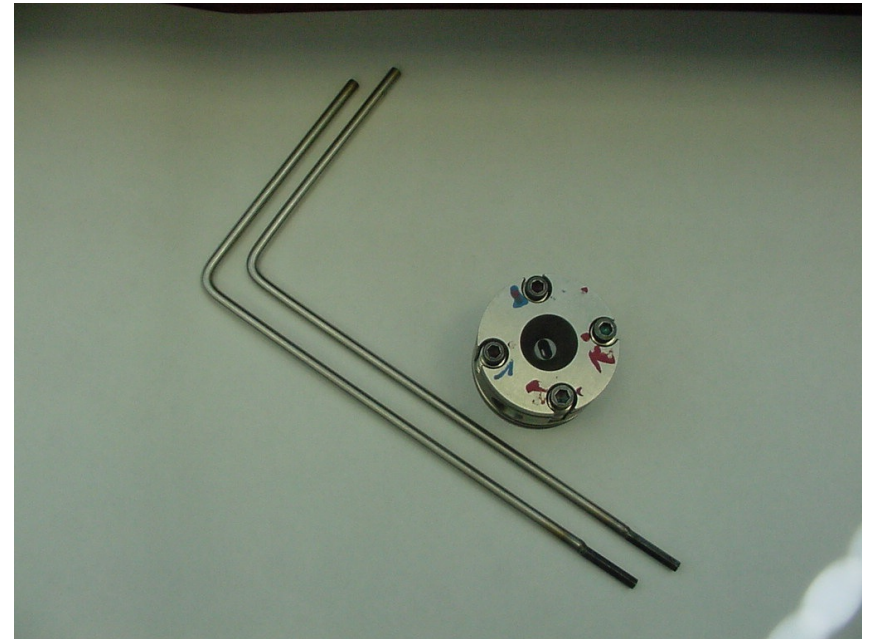


- Cover**
- Membrane**
- Interface disk**
- Upper carbide tungsten rocker**
- Upper rocker support (movable)**
- Guidance pin**
- Gasket (Stainless steel or rhenium)**
- Lower carbide tungsten rocker**
- Lower rocker support (fixed)**



Height : 32 mm  
Diameter : 50 mm

# Screw driver (Hand) driven DAC



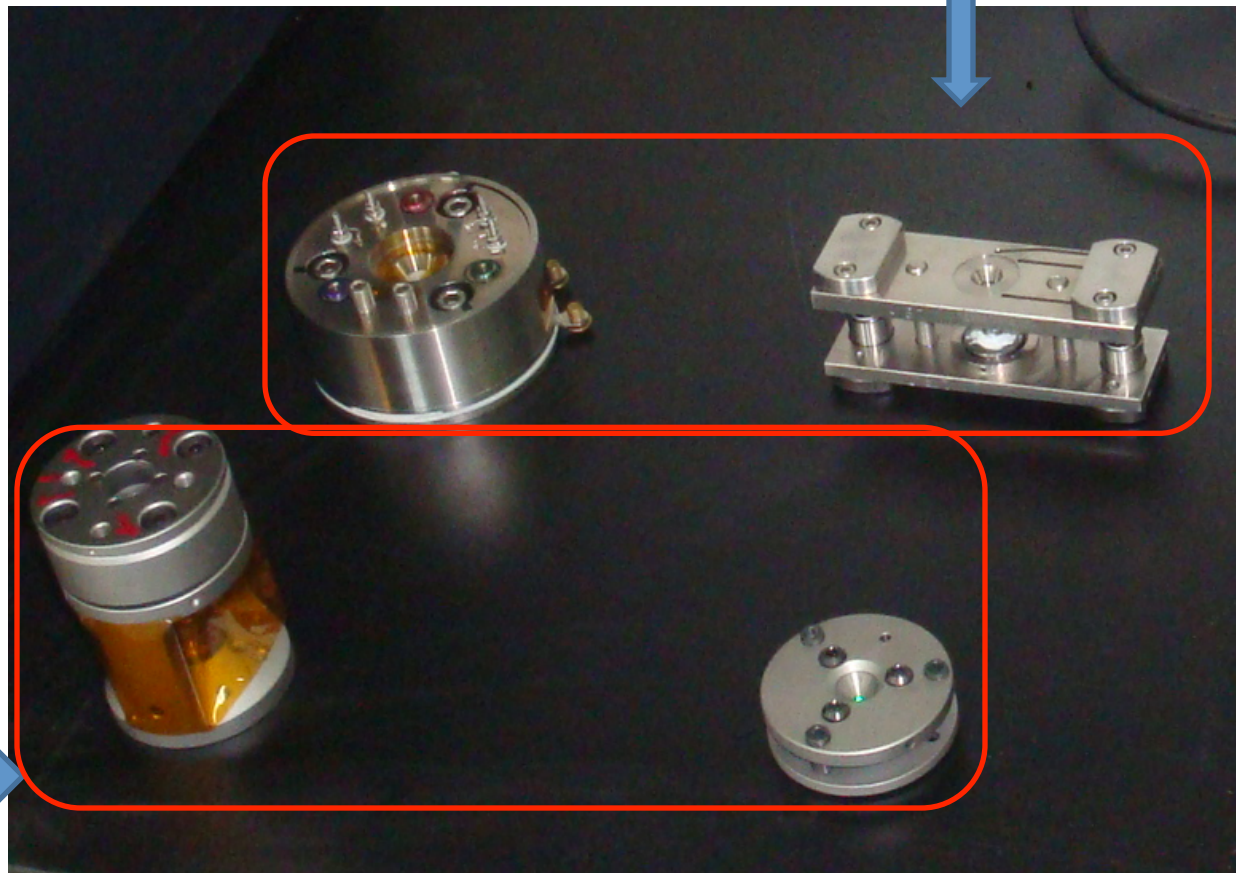
# DACs

Hydrothermal cells

~160 degree side opening angle



Typical symmetric cells

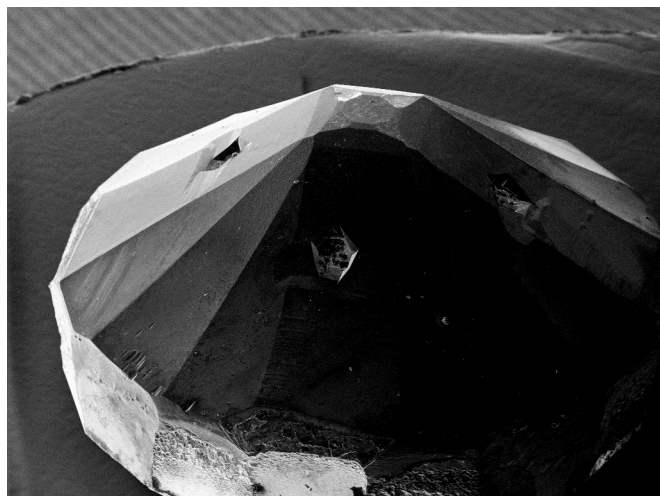


~140 degree side opening angle

Panoramic cell

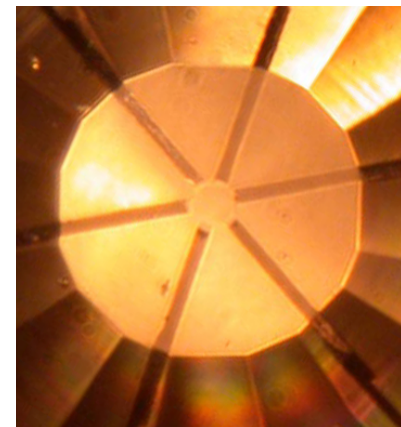
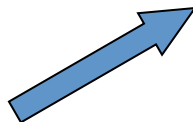
Plate cell

# A Powerful and Versatile High-P Technology

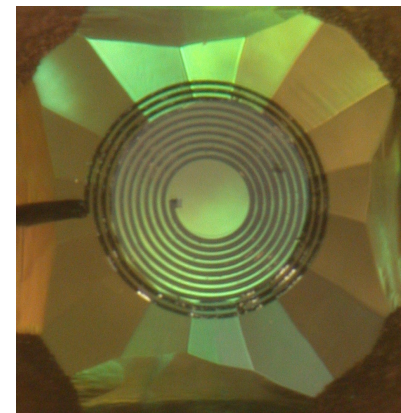


*Designer Diamond Anvil*

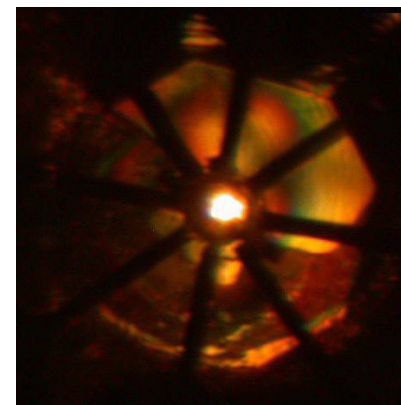
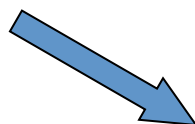
Electrical Conductivity  
Experiments



Magnetic Susceptibility  
Experiments



High-P/High-T  
Experiments



# *In situ* Research under High Pressure

- Lab XRD
- Raman
- IR
- Brillouin
- Absorption
- Electronic and Magnetic Measurement
- ...

- Synchrotron & neutron sources

Dedicated & non-dedicated high pressure stations

XRD

Imaging

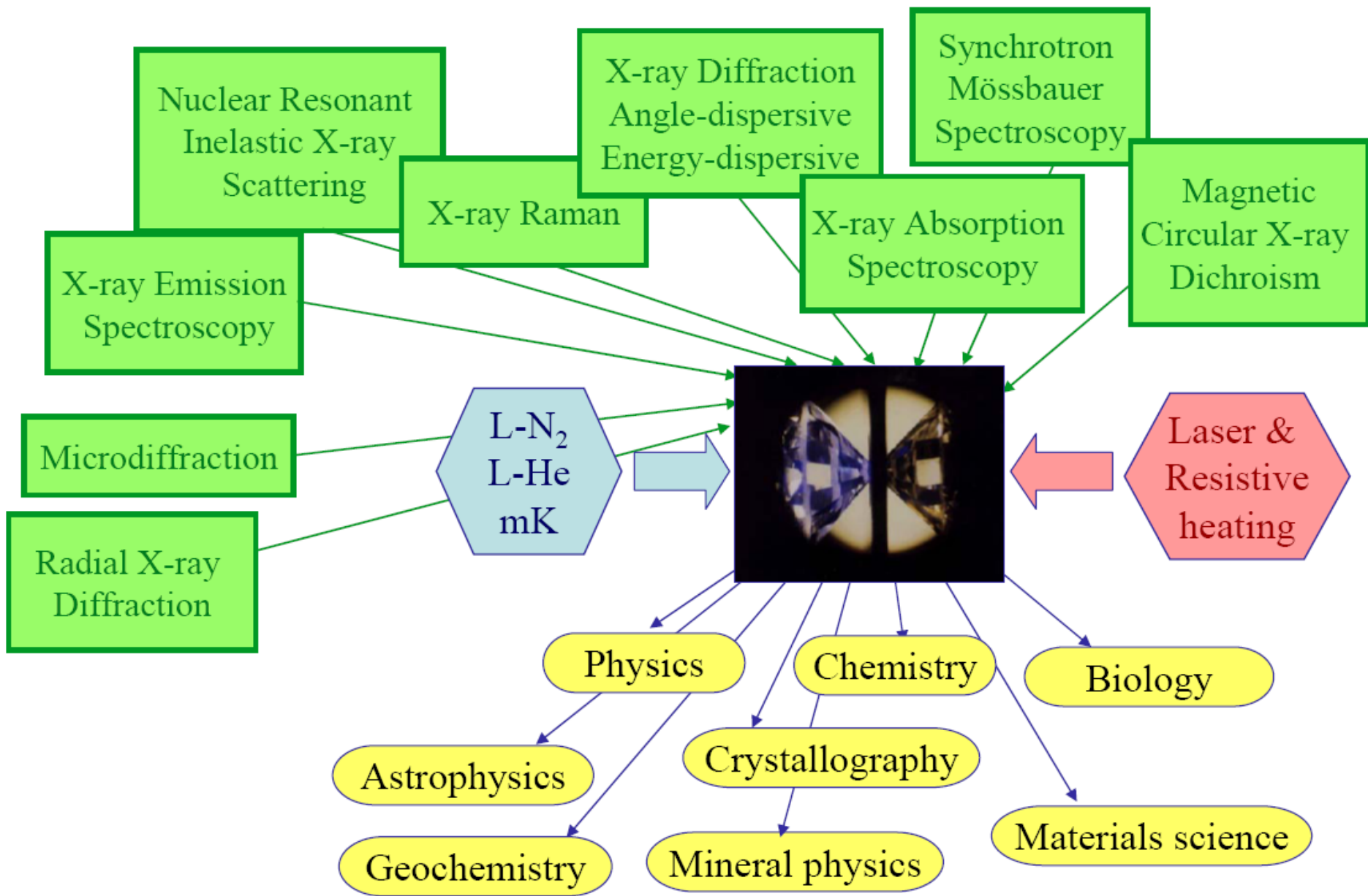
IXS

PDF

SAS, WAS

ESAF

...

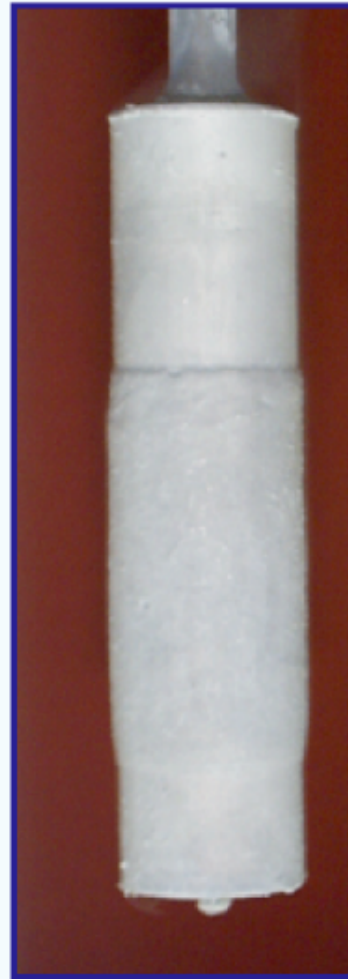
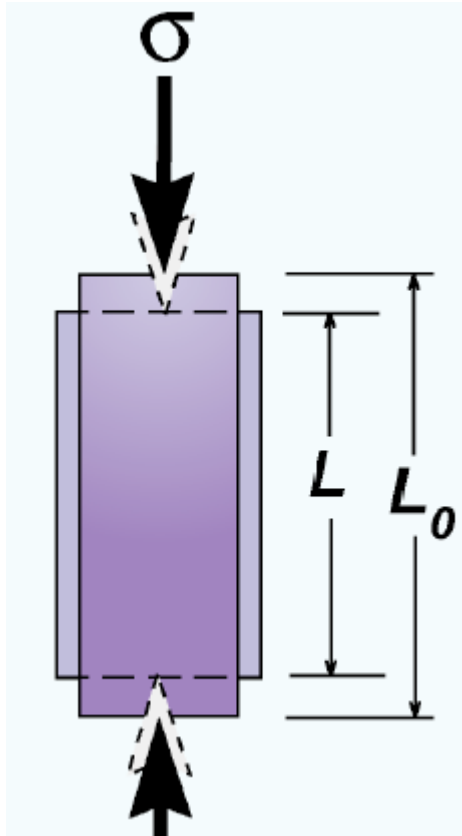


# High pressure measurement & calibration

- Force
- Area
- Pressure measurement
  
- Higher pressure: totally different story!

$$P=F/A$$

# Deformation



- Free rotation piston-cylinder (deformation free condition)

# Pressure calibration: Goal

## Primary calibration (accuracy)

1- 100 GPa  $\Delta P/P = \pm 1\%$

100- 300 GPa  $\Delta P/P = \pm 1\%$

High temperatures --

at 100 GPa-2500 K  $\Delta P/P = \pm 1\%$

## Secondary calibration (precision)

10 MPa – 1 GPa  $\Delta P = \pm 5$  MPa

1- 100 GPa  $\Delta P/P = \pm 0.2\%$

100- 300 GPa  $\Delta P/P = \pm 0.2\%$

Primary calibration requires measurements of two independent functions related to pressure.

## Examples:

- $F$  and  $A$  – free rotation piston-cylinder
- $U_S$  and  $U_P$  – shock Hugoniot
- $V_\phi$  and  $\rho$  – DAC or LVP

$$V_\phi^2 = K/\rho$$

$$K = \rho dP/d\rho$$

$$P = \int V_\phi^2 d\rho.$$

## Techniques involve

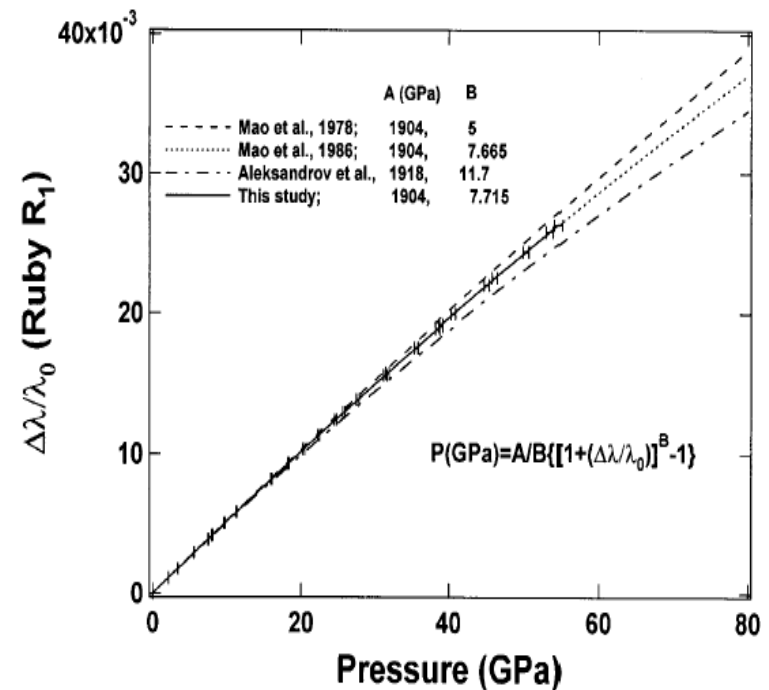
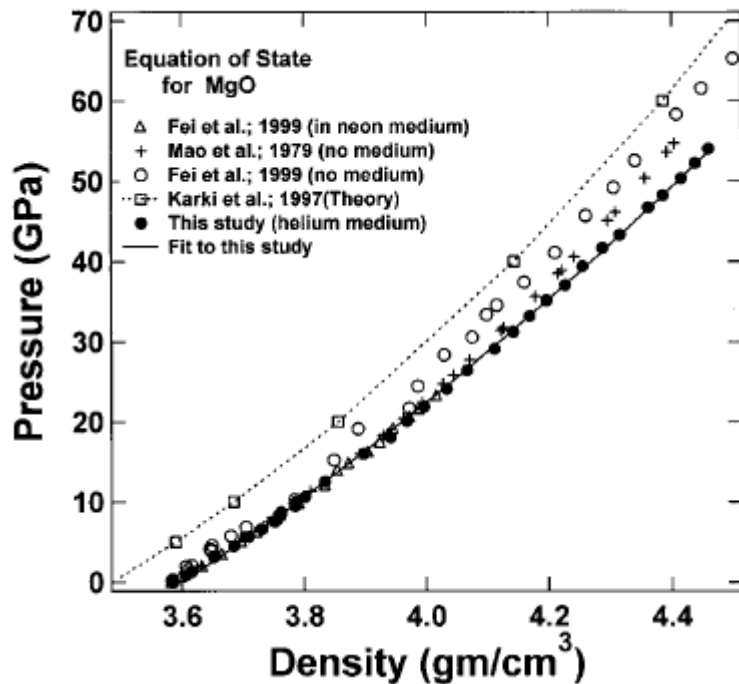
- X-ray diffraction (axial and radial)
- Optical spectroscopy (Brillouin, Raman, fluorescence)
- Ultrasonic measurement
- Inelastic x-ray scattering spectroscopy

# Pressure calibration, $\Delta P/P \pm 1\%$

Zha, Mao, Hemley, *PNAS* (2000)

$\rho$  from x-ray diffraction  
 $V_\phi$  from Brillouin scattering  
 $P$ - $\rho$  EOS by integration (Primary)

Ruby fluorescence shift  
Calibrated by MgO  $P$ - $\rho$  EOS  
(Secondary)



## Elasticity Grand Challenge

### COMPRES Infrastructure Development Project

Measure sound velocities and density simultaneously

“Absolute” or internally consistent Pressure Scales  
Zha et al., Brillouin on MgO (PNAS, 2000)

Isothermal bulk modulus  
(volume measurements)

$$K = -V \left( \frac{dP}{dV} \right)$$

$$P = - \int_{V_0}^V \frac{K(V)}{V} dV$$

Adiabatic elastic moduli  
(velocity measurements)

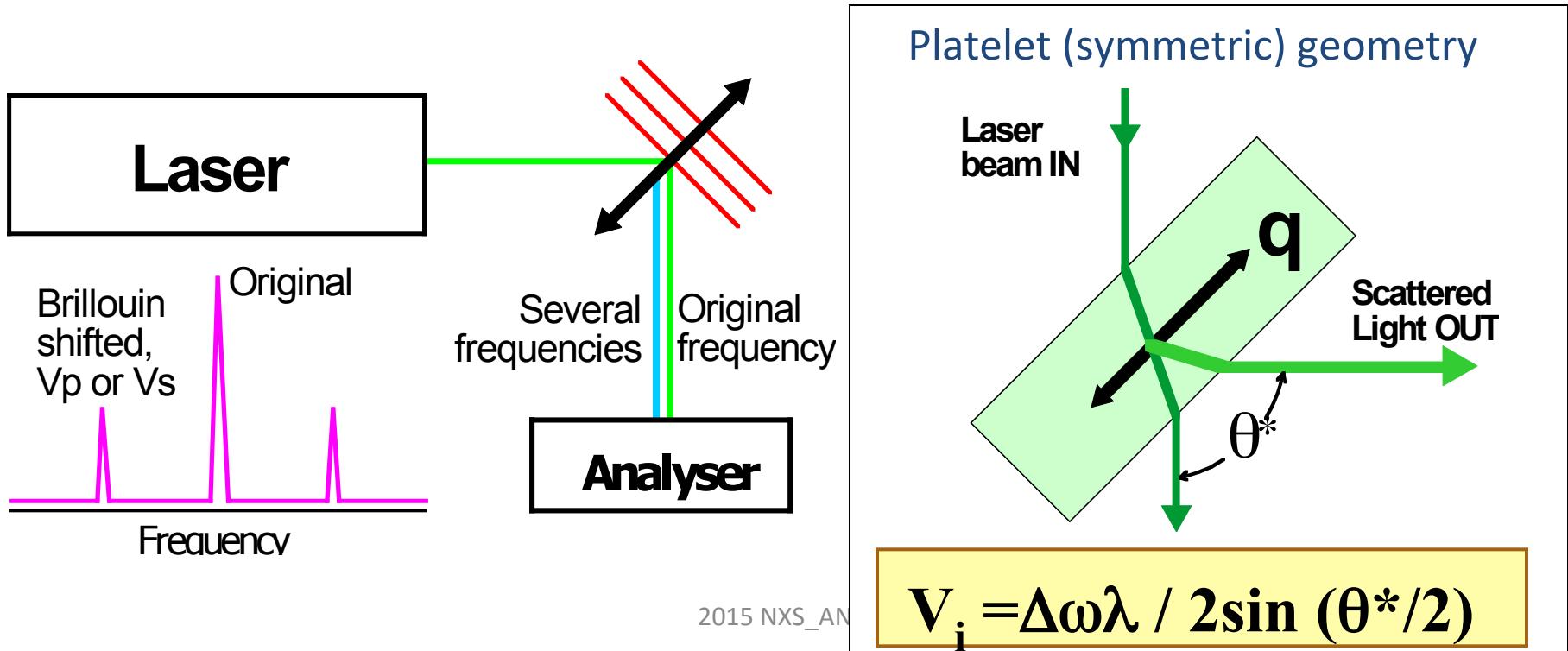
$$\mu = \rho V_S^2$$

$$K = \rho V_P^2 - (4/3)\rho V_P^2$$

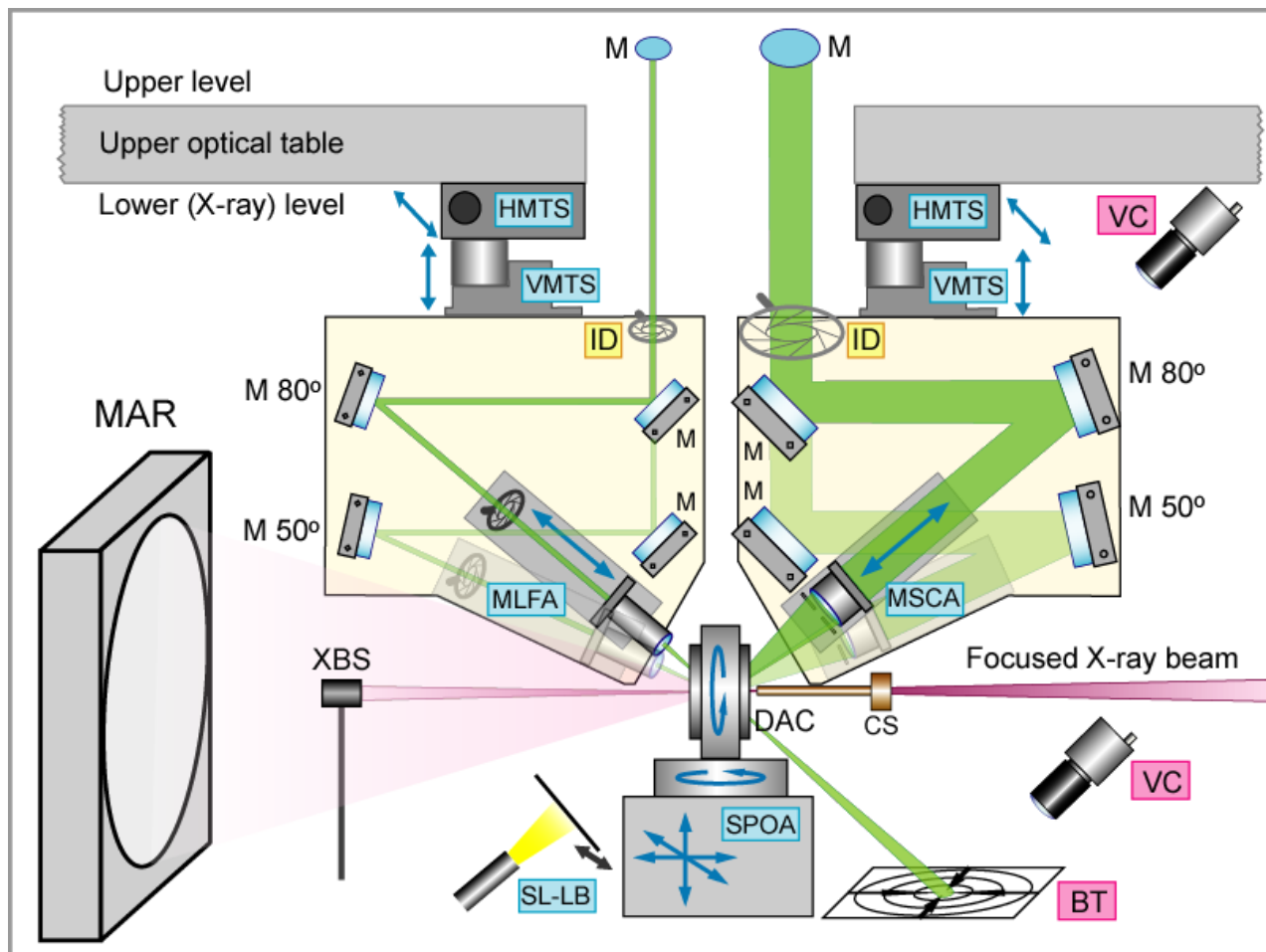
# Brillouin scattering

- **Acoustic waves** present in a solid due to **thermal motion of atoms**
- **Laser light interacts with phonons** (or density / refractive index fluctuations) and is **scattered with Doppler shifted frequency  $\Delta\omega$**
- Brillouin shift is **proportional to acoustic velocity**

$$V_i = \Delta\omega\lambda / 2n \sin(\theta/2)$$



# Schematic diagram of the Brillouin system installed at sector 13-BMD at APS



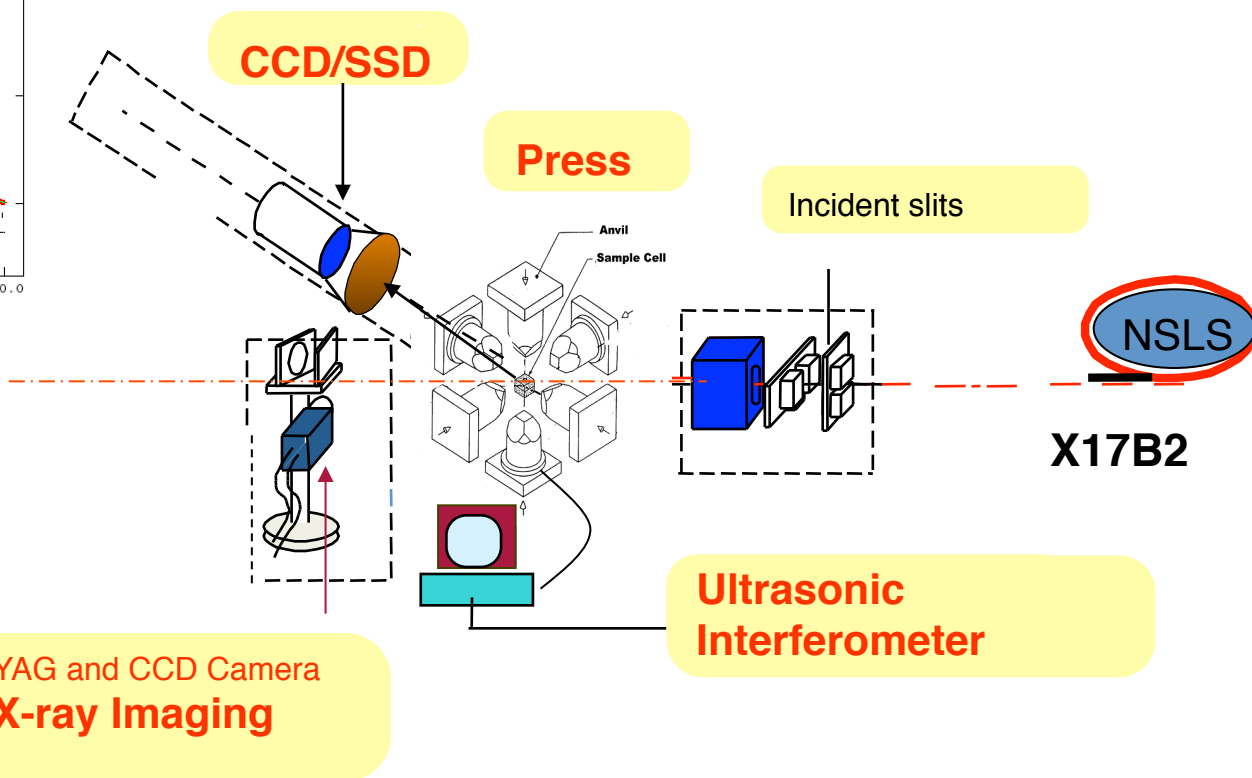
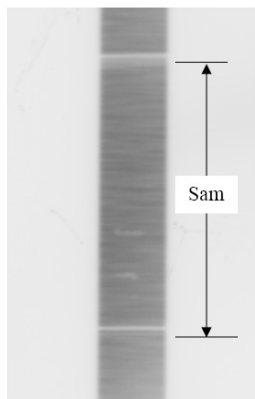
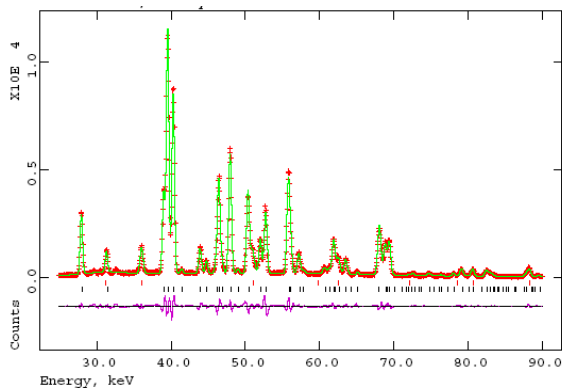
**Motorized translation components (controllable from outside the hatch, blue boxes):** HMTS - horizontal motorized translation stage; VMTS - vertical motorized translation stage; MLFA - motorized laser focusing assembly; MSCA - motorized signal collecting assembly; SPOA - sample positioning and orientation assembly; SL-LB - sample light / light block.

**Observation / feedback elements (red boxes):** VC - video camera; BT - beam target.

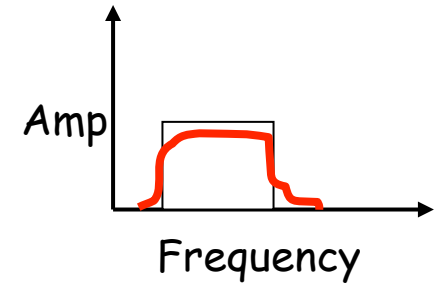
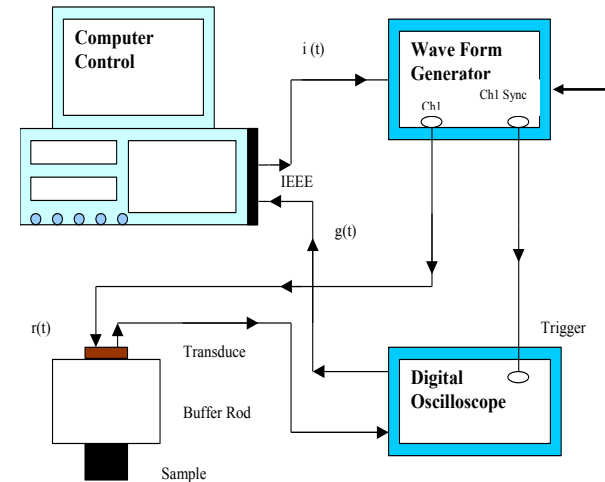
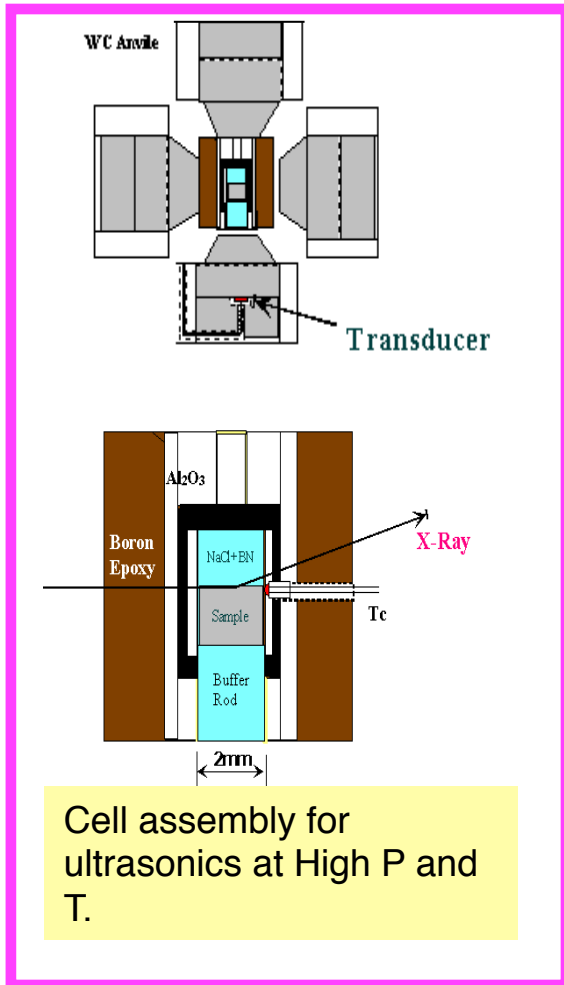
**X-ray components:** MAR - MAR Imaging plate; XBS - X-ray beam stop; CS - cleanup slit.

# High Pressure Ultrasonic Experimental Techniques

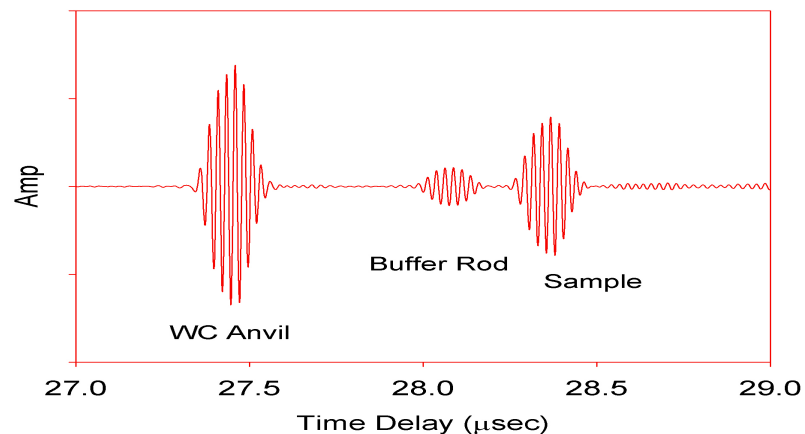
## Simultaneous P-V-T Eos and Sound Velocity ( $V_p, V_s$ ) Measurements



# Ultrasonic Interferometry

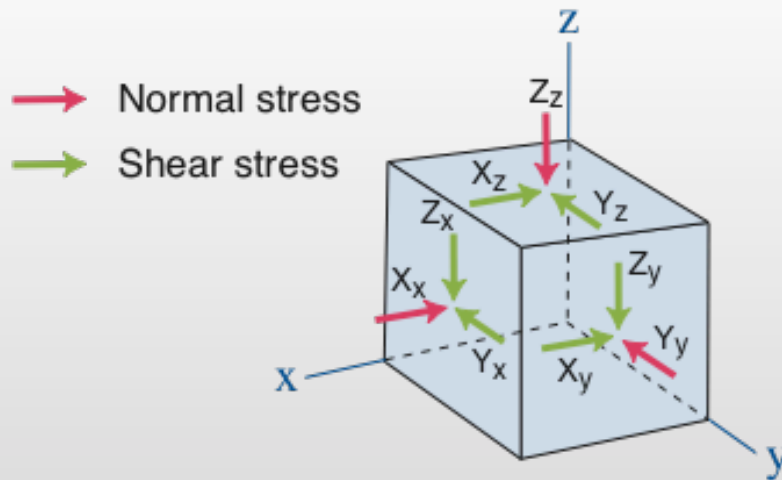


P and S wave travel times ( $t_p$ ,  $t_s$ ) inside the sample are measured at the same time



“Pressure” is meaningful only under hydrostatic conditions.

## Stress tensor



	Stress		Spatial
	Shear	Differential	Inhomogeneity
Nonhydro.	○	○	○
Uniaxial	—	○	—
Hydro.	—	—	—

Nonhydrostatic

$$\begin{pmatrix} X_x & X_y & X_z \\ Y_x & Y_y & Y_z \\ Z_x & Z_y & Z_z \end{pmatrix}$$

Uniaxial

$$\begin{pmatrix} X_x & 0 & 0 \\ 0 & Y_y & 0 \\ 0 & 0 & Z_z \end{pmatrix}$$

Hydrostatic

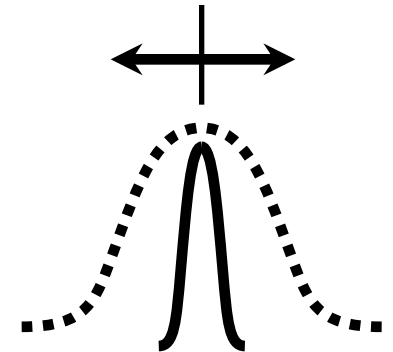
$$\begin{pmatrix} P & 0 & 0 \\ 0 & P & 0 \\ 0 & 0 & P \end{pmatrix}$$

Nonhydrostatic stress conditions are difficult to reproduce ...

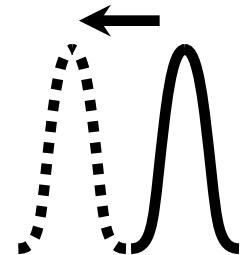
$$X_x = Y_y \neq Z_z$$

# Nonhydrostatic stress

- Stress inhomogeneity (signal)  
pressure gradients  $\longleftrightarrow$  broadening



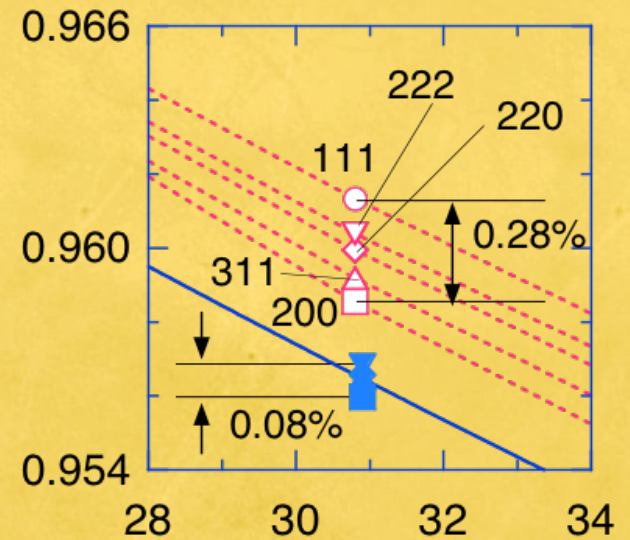
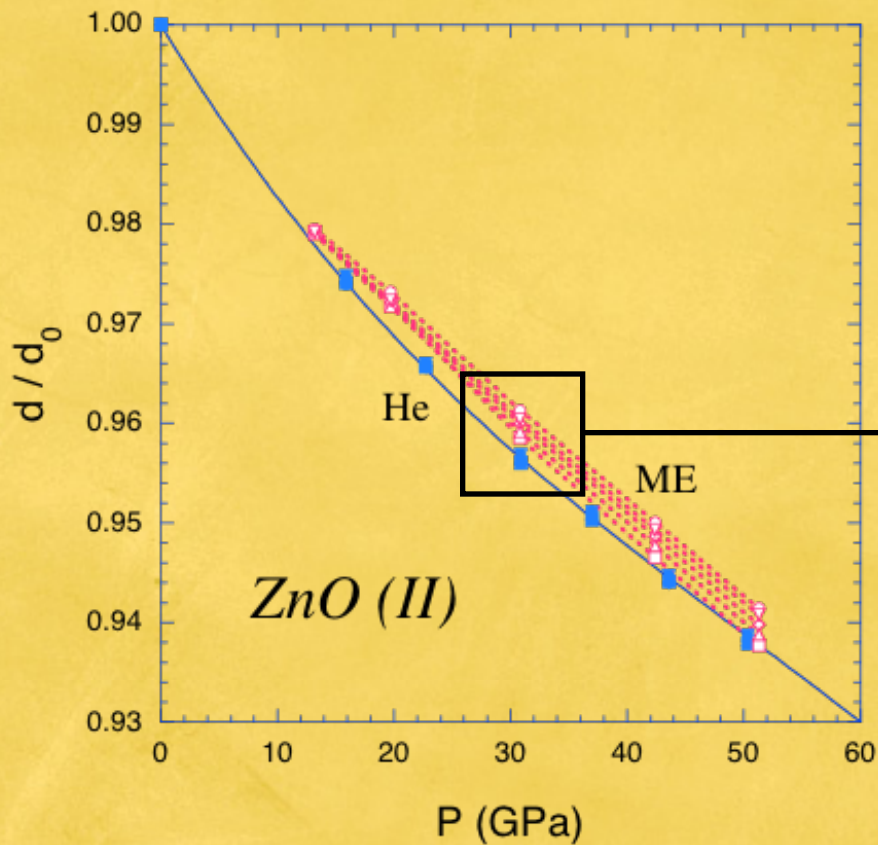
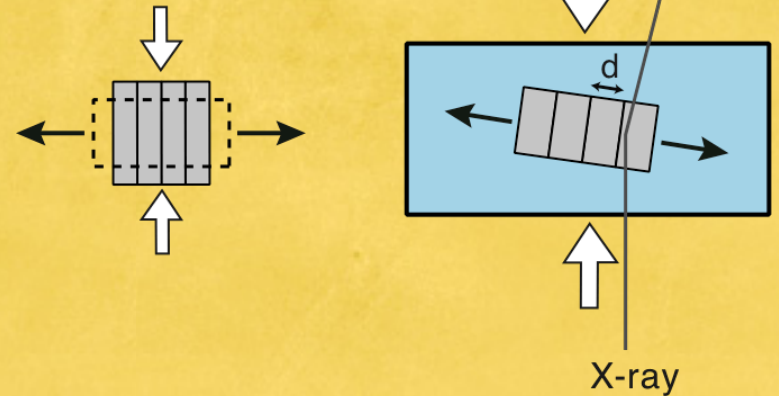
- Uniaxial stress (signal)  
lattice distortion  $\longleftrightarrow$  shift



more serious !

# Deformation under uniaxial stress

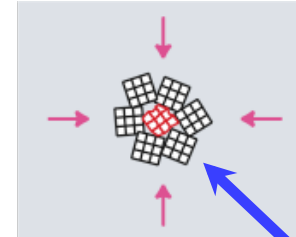
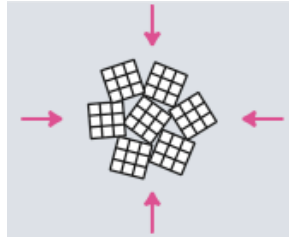
Poisson's effect



K. Takemura, JAP **89**, 662 (2001).

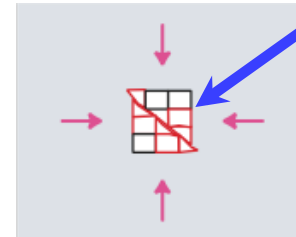
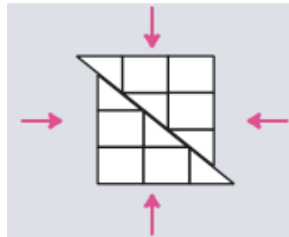
# Local stress

polycrystalline

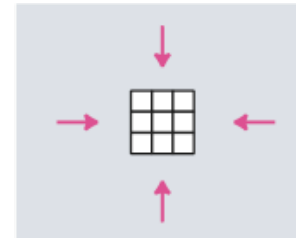
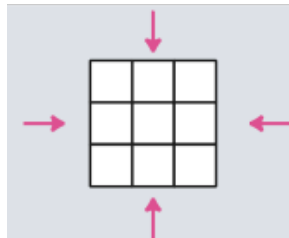


local stress !  
broadening

single crystal  
(+ grain boundaries,  
dislocations, twins, ...)



single crystal



Ideal hydrostatic conditions can only be achieved with a fluid pressure medium and a perfect single crystal.

# In practice, pressure was measured:

- Powder XRD *via* well-known EoS of markers (Pt, Au,...)
- Ruby pressure scale

Secondary pressure calibration!!

# Fluorescent spectroscopy

- Ruby ( $\text{Al}_2\text{O}_3$ ),  $\text{YAlO}_3$ , YAG, MgO, and a few others.
- Ruby's main fluorescence lines (the R1 R2 doublet) were intense and sharp, and the lines shifted measurably toward the red with increasing pressure

R. A. Forman, G. J. Piermarini, J. D. Barnett, and S. Block, Pressure Measurement Made by the Utilization of Ruby Sharp-Line Luminescence, *Science* **176**, 284 (1972).

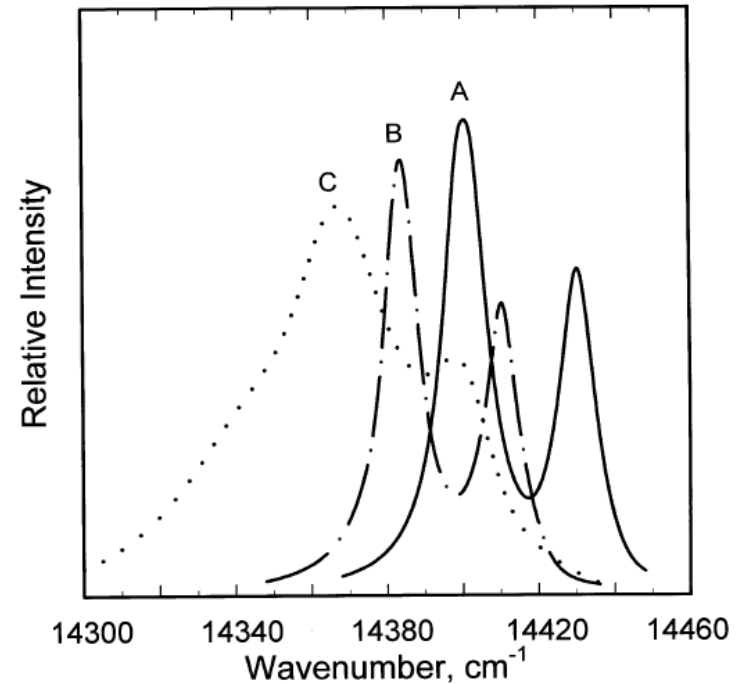


Fig. 20. The R-line luminescence spectra of a crystal of ruby in the diamond anvil cell at room temperature. Ruby crystal: at ambient pressure (A); at about 2.23 GPa (22.3 kbar) hydrostatic pressure (B); and at an average nonhydrostatic pressure of about 4 GPa (40 kbar) (C). Effects of a hydrostatic pressure-shift and line-sharpening (A)-to-(B), and nonhydrostatic pressure-shift and line-broadening (A)-to-(C), are illustrated in this figure. The pressure-shift is to lower energy (toward the red) with increasing pressure.

- H. K. MAO and P. M. BELL, High-Pressure Physics: The 1-Megabar Mark on the Ruby *R1* Static Pressure Scale, *Science*, Vol. 191. no. 4229, pp. 851 – 852, 1976
- H. K. MAO and P. M. BELL, High-Pressure Physics: Sustained Static Generation of 1.36 to 1.72 Megabars, *Science* 200, 1145-1147 1978
- H.-K. Mao, J. Xu, and P. M. Bell, *J. Geophys. Res.* 91, 4673 (1986).

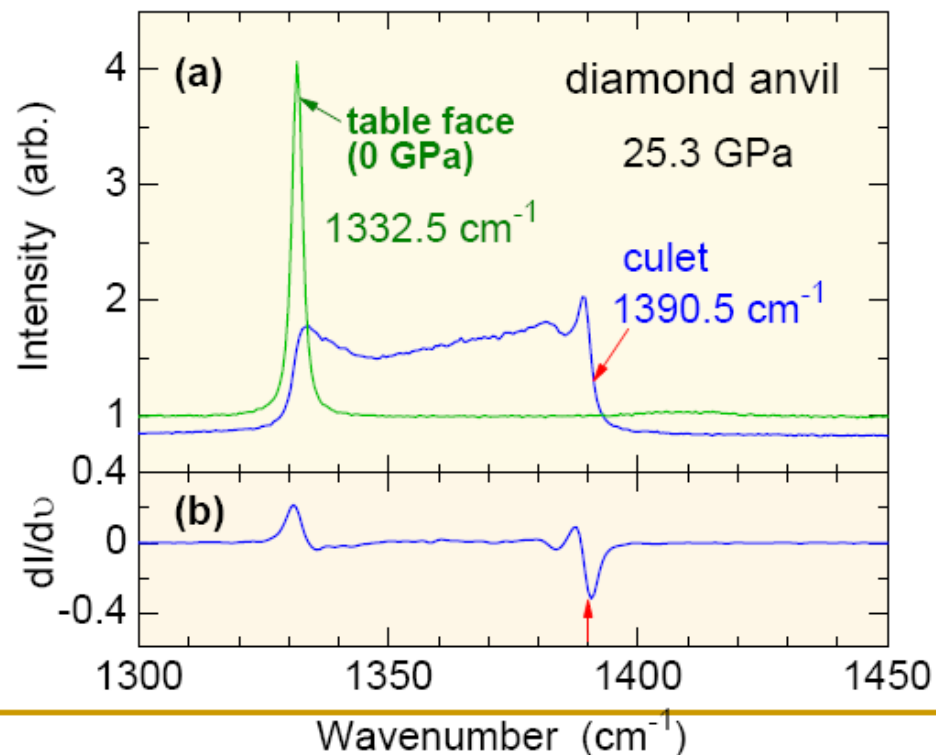
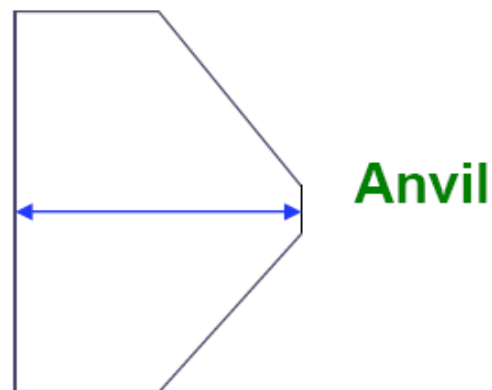
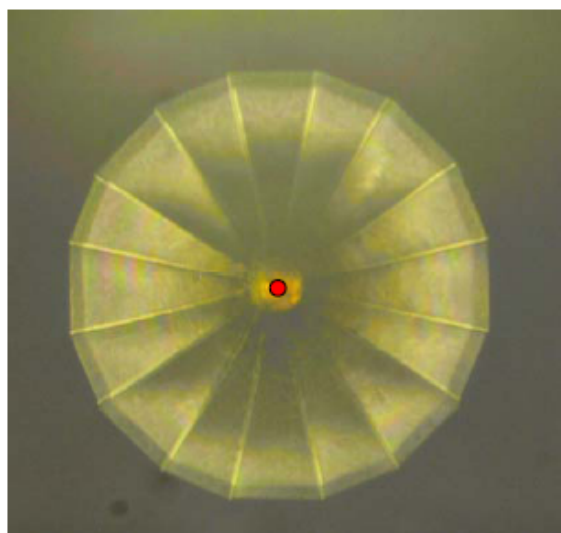
$$P = \frac{A}{B} \left[ \left( \frac{\lambda}{\lambda_0} \right)^B - 1 \right]$$

with  $A = 1904$ ,  $B = 7.665$

# Diamond anvil Raman Spectroscopy

Hanfland&Syassen(1985)

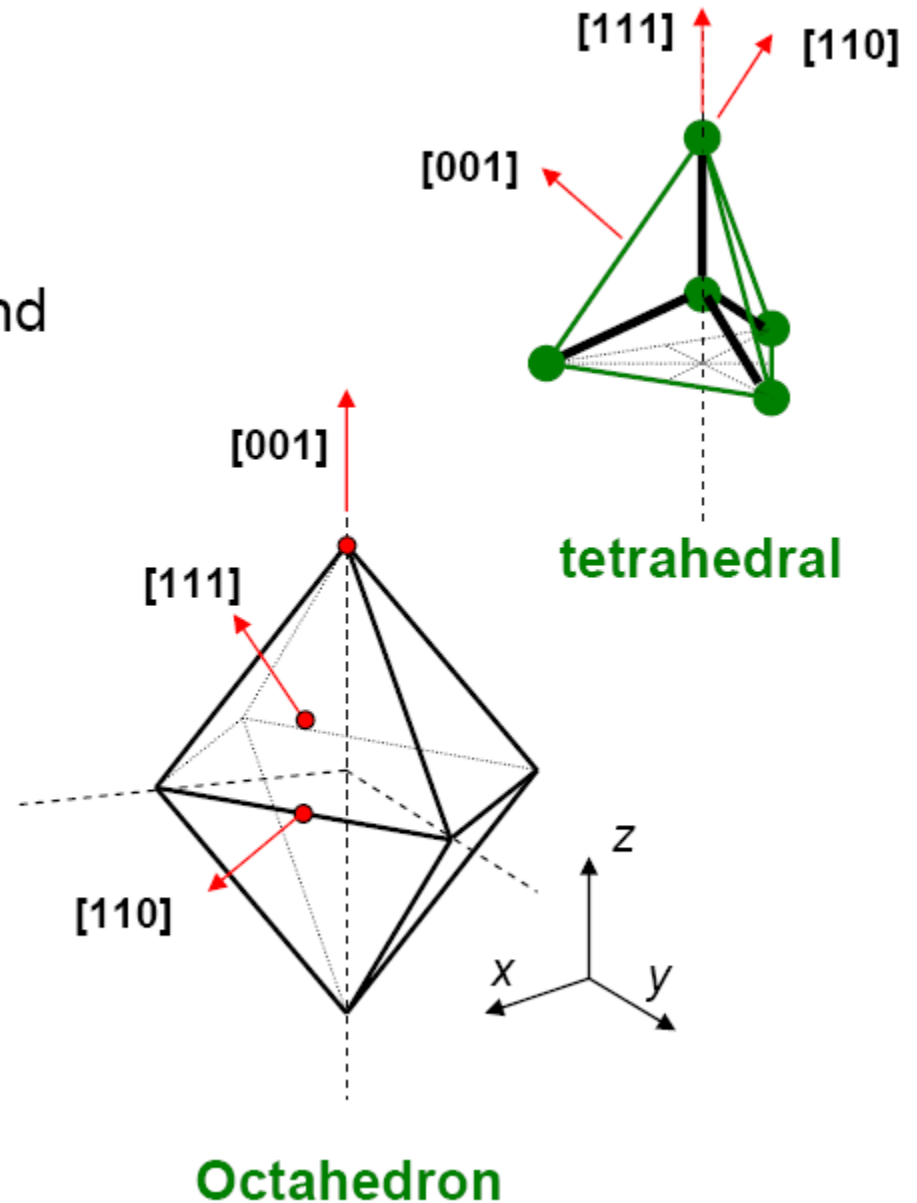
The first-order Raman mode:  
 $F_{2g}$  optical phonon



# Load axis of diamond anvils

- Pressure calibration for diamond anvil Raman gauge
  - Load axis: [001] direction  
[001] anvil
- Stress state analysis
  - Load axis: [111], [110]  
[111] or [110] anvil

Anisotropy of hardness  
Pressure generation



# Diamond anvil Raman gauge

## 1. [001] anvil: Pressure calibration of Raman edge with Pt-EOS to 370 GPa

$P \leq 300$  GPa

$$P(\text{GPa}) \cong 547 \frac{\Delta\nu}{\nu_0} \left[ 1 + \frac{1}{2} (3.75 - 1) \frac{\Delta\nu}{\nu_0} \right] \quad \text{Pressure error: 3\%}$$

$P \geq 200$  GPa

$$P(\text{GPa}) = 3141 - 4.157\nu + 1.429 \times 10^{-3} \nu^2 \quad \text{Pressure error: 2\%}$$

useful method for pressure determination in the multimegabar range

## 2. [111] & [110] anvils: Direct observation of stress state

Obtained pressure dependence of shear stress ( $\tau$ )

suggested possibility of pressure generation beyond 400GPa

# Equation of State (EoS)

- The relationships among the pressure, the volume, and the temperature are described by the Equation of State (EoS).
- Ideal gas:  $PV=nRT$

- The volume-temperature relationship is described by the definition of the volume coefficient of expansion

$$\alpha_{Vp} \equiv \frac{1}{V} \left( \frac{\partial V}{\partial T} \right)_p$$

- The relationship between the pressure and the volume is given by the isothermal bulk modulus

$$B_T \equiv -V \left( \frac{\partial p}{\partial V} \right)_T$$

### Conditions

For the validity of equation, it is assumed that the solid is homogeneous, isotropic, nonviscous and has linear elasticity. It is also assumed that the stresses are isotropic; therefore, the principal stresses can be identified as the pressure

$$p = \sigma_1 = \sigma_2 = \sigma_3 .$$

A universal EoS must cover the entire pressure and temperature range; therefore, it is necessary to incorporate all of the derivatives of the volume coefficient of expansion and the isothermal bulk modulus. There is no single expression known for universal!

$$\left(\frac{\partial\alpha_V}{\partial T}\right)_p ; \left(\frac{\partial\alpha_V}{\partial p}\right)_T ; \left(\frac{\partial B_T}{\partial T}\right)_p ; \left(\frac{\partial B_T}{\partial p}\right)_T$$

- The determined values of the volume and the bulk modulus at temperature T can be used as initial parameters for an isothermal EoS.
- The isothermal equation of states follow finite strain, interatomic potential, or empirical approach.

## Finite-strain EoS

- The Birch-Murnaghan EoS (Birch, 1947; Murnaghan, 1937, 1944) assumes that the strain energy of a solid can be expressed as a Taylor series in the finite Eulerian strain. Expansion to fourth order in the strain yields an EoS:

$$p = 3B_0 f_E (1 + 2f_E)^{\frac{5}{2}} \left\{ 1 + \frac{3}{2}(B'-4)f_E + \frac{3}{2} \left[ B_0 B'' + (B'-4)(B'-3) + \frac{35}{9} \right] f_E^2 \right\}$$
$$f_E = \frac{\left( \frac{V_0}{V} \right)^{\frac{2}{3}} - 1}{2}$$

# The most widely used isothermal EoS

$$P(V) = \frac{3B_0}{2} \left[ \left( \frac{V_0}{V} \right)^{\frac{7}{3}} - \left( \frac{V_0}{V} \right)^{\frac{5}{3}} \right] \left\{ 1 + \frac{3}{4} (B'_0 - 4) \left[ \left( \frac{V_0}{V} \right)^{\frac{2}{3}} - 1 \right] \right\}$$

## Third order Birch EoS

- F.D. Murnaghan, 'The Compressibility of Media under Extreme Pressures', in *Proceedings of the National Academy of Sciences*, vol. 30, pp. 244-247, 1944.
- Francis Birch, 'Finite Elastic Strain of Cubic Crystals', in *Physical Review*, vol. 71, pp. 809-824 (1947).

## *Inter-atomic potential EoSs*

- The theoretical base for the interatomic potential EoS lays in the thermodynamic relationship

$$p = T \left[ \frac{\partial p}{\partial T} \right]_V - \left[ \frac{\partial U}{\partial V} \right]_{T,m}$$

$$P = - \left( \frac{\partial E}{\partial V} \right)_S \quad E = E_0 - \int P dV$$

$$E(V) = E_0 + \frac{9V_0 B_0}{16} \left\{ \left[ \left( \frac{V_0}{V} \right)^{\frac{2}{3}} - 1 \right]^3 B'_0 + \left[ \left( \frac{V_0}{V} \right)^{\frac{2}{3}} - 1 \right]^2 \left[ 6 - 4 \left( \frac{V_0}{V} \right)^{\frac{2}{3}} \right] \right\}$$

The potential function proposed by Mie and extended by Grunesisen

$$U(r) = -\frac{A}{r^m} - \frac{B}{r^n} = -\frac{A}{V^{\left(\frac{m}{3}\right)}} + \frac{B}{V^{\left(\frac{n}{3}\right)}}$$

$$p = \frac{3K_T(0)}{m-n} \left[ \left( \frac{V_o}{V} \right)^{\left(\frac{m+3}{3}\right)} - \left( \frac{V_o}{V} \right)^{\left(\frac{n+3}{3}\right)} \right]$$

“Universal EoS” derived by Rose from a general inter-atomic potential (Rose, 1984) which was promoted by (Vinet, 1987-a, -b) is also commonly used:

$$p = 3K_0 \frac{1 - f_V}{f_V^2} e^{\left[ \frac{3}{2}(B'-1)(1-f_V) \right]}$$

$$f_V = \left( \frac{V}{V_0} \right)^{\frac{1}{3}}$$

The Vinet EoS gives very accurate results for simple solids at very high pressure.

# *Empirical EoS*

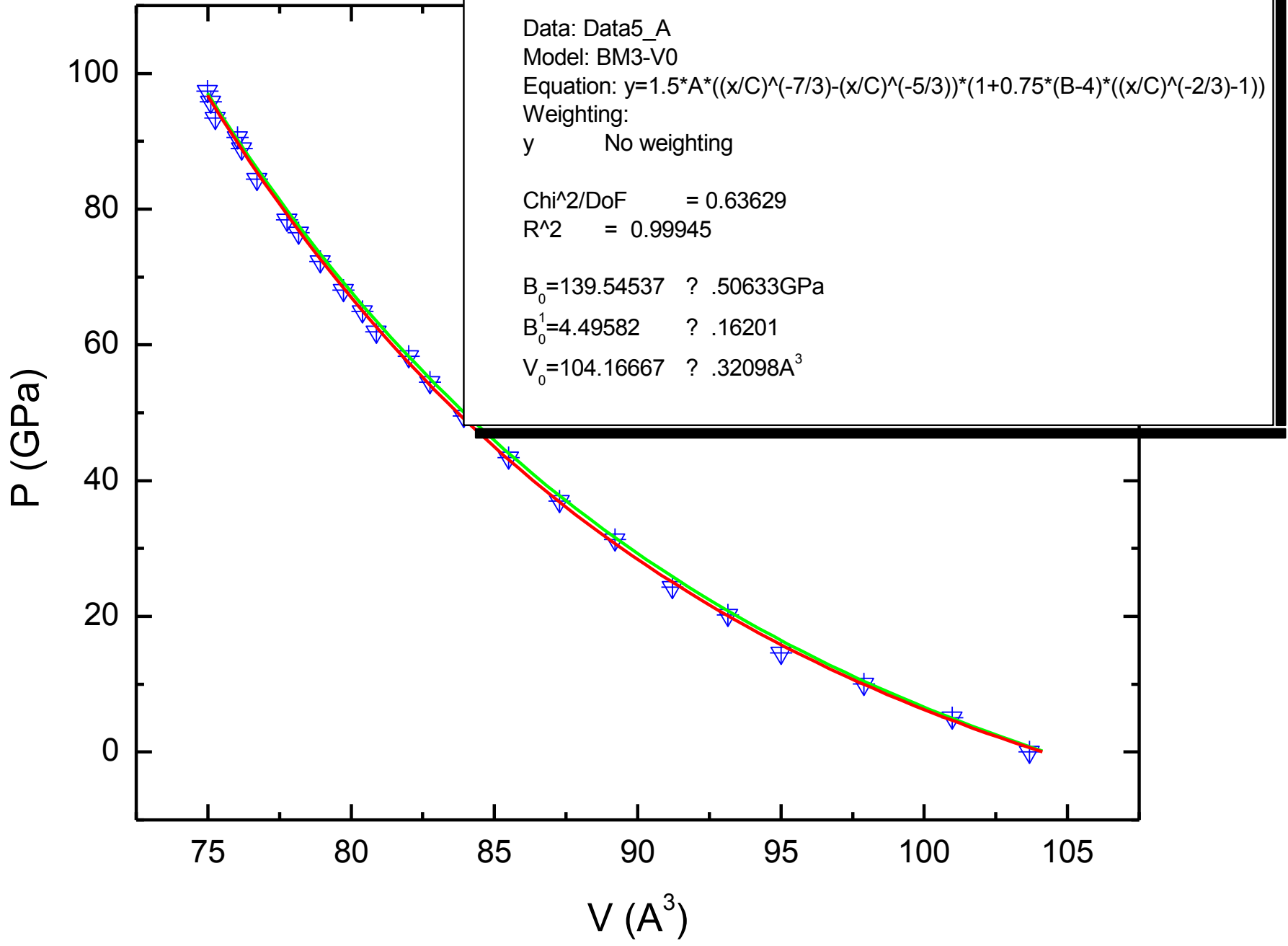
- Find a mathematical function which gives the best fit to the experiments

$$V = V_0 \left[ 1 - \frac{\ln(1 + ap)}{b + cp} \right]$$

$$a = \frac{1}{8B_0} \left[ 3(B_0' + 1) + (25B_0'^2 + 18B_0' - 32B_0B_0'' - 7)^{\frac{1}{2}} \right]$$

$$b = \frac{1}{8} \left[ 3(B_0' + 1) + (25B_0'^2 + 18B_0' - 32B_0B_0'' - 7)^{\frac{1}{2}} \right]$$

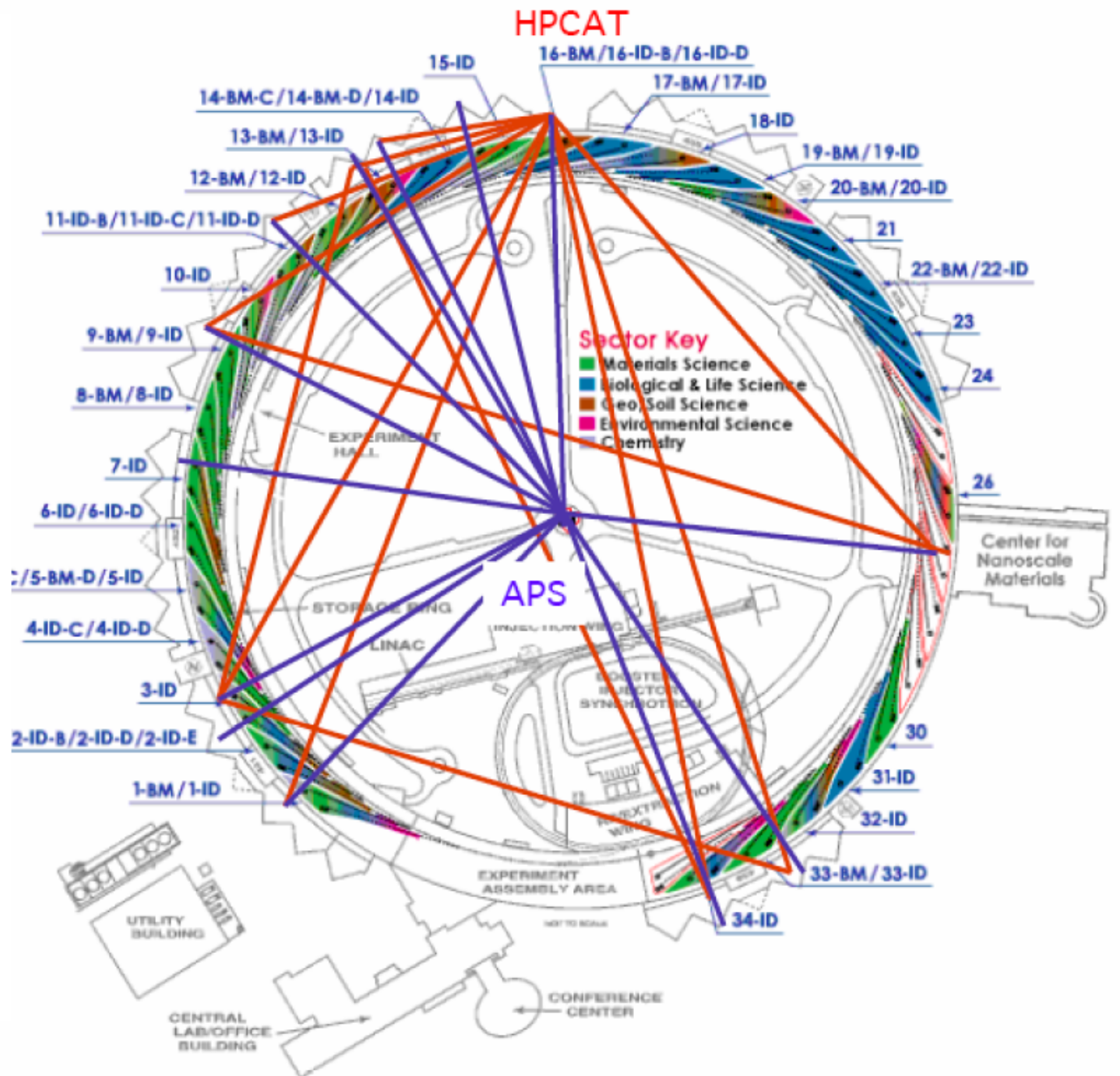
$$c = \frac{1}{16} \left[ 3(B_0' + 1) + (25B_0'^2 + 18B_0' - 32B_0B_0'' - 7)^{\frac{1}{2}} \right] (B_0' + 1) - \frac{1}{8} \left[ 3(B_0' + 1) + (25B_0'^2 + 18B_0' - 32B_0B_0'' - 7)^{\frac{1}{2}} \right]$$



## Bulk Moduli for CdO

Structural Type	$K_0$ (GPa)	$K'_0$	Pressure range (GPa)	Pressure marker	Pressure medium	Techniques	Reference
B1	$150 \pm 1$	4 (fixed)	0-9.7	Ruby	Methanol-ethanol	ADXRD /DAC	This work run #1
	$147 \pm 4$	$4.2 \pm 0.1$	0-89	Au	None	ADXRD /DAC	This work run #2
	$148 \pm 1$	4 (fixed)	0-8.1	NaCl	BN	EDXRD /LVC	Ref. [13], 1999
	$150 \pm 1$	4 (fixed)	0-7.8				
	108	9	0-35	NaCl, Ag, MgO	NaCl, Ag, MgO	XRD/DP	Ref. [11], 1966
	130	4.13	--	--	--	Calculation /GGA	Ref. [9], 2002
B2	$169 \pm 7$	4.66 (fixed)	102-176	Au	None	ADXRD /DAC	This work run #2
	114	4.66	--	--	--	Calculation /GGA	Ref. [9], 2002

# HP-SynC



# X RAYS AND CRYSTAL STRUCTURE

BY  
W. H. BRAGG, M.A., D.Sc., F.R.S.  
CAVENDISH PROFESSOR OF PHYSICS, UNIVERSITY OF LEEDS

AND  
W. L. BRAGG, B.A.  
FELLOW OF TRINITY COLLEGE, CAMBRIDGE



LONDON  
G. BELL AND SONS, LTD.

1915

## ANALYSIS OF CRYSTALS

173

CRYSTAL.	A.	SYSTEM.	REMARKS.
Diamond, C ... ..	...	cubic.	
Copper, Cu ... ..	...	"	Atoms of Cu on face-centred cubic lattice.
{ Sodium chloride, NaCl ... ..	...	"	
{ Potassium chloride, KCl ... ..	...	"	
{ Potassium bromide, KBr ... ..	...	"	
{ Potassium iodide, KI ... ..	...	"	
Galena, PbS ... ..	...	"	Pb and S as Na and Cl in sodium chloride.
Zinblende, ZnS ... ..	...	"	
Zincite, ZnO ... ..	...	hexagonal.	} Two interpenetrating hexagonal lattices.
Cadmium sulphide, CdS ... ..	...	"	
Fluor, CaF <sub>2</sub> ... ..	...	cubic.	
{ Pyrites, FeS <sub>2</sub> ... ..	...	"	
{ Hauerite, MnS <sub>2</sub> ... ..	...	"	
{ Sodium nitrate, NaNO <sub>3</sub> ... ..	...	rhombohedral.	
{ Calcite, CaCO <sub>3</sub> ... ..	...	"	
{ Dolomite, CaMg(CO <sub>3</sub> ) <sub>2</sub> ... ..	...	"	
{ Rhodochrosite, MnCO <sub>3</sub> ... ..	...	"	
{ Chalybite, FeCO <sub>3</sub> ... ..	...	"	



# ZnO under high pressure

- Am. Psychol. 13, 334 (abstract) (1958).
8. C. W. Jackson, Jr., and E. L. Kelly, *Science* 135, 211 (1962).
9. W. Dement and N. Kleinman, *Electroencephalogr. Clin. Neurophysiol.* 9, 673 (1953).
10. D. R. Goudeonough and H. B. Lewis, department of psychiatry, College of Medicine, State University of New York, personal communications.
11. H. Kluver, *Proc. Assoc. Res. Nervous and Mental Diseases* 14, 150 (1933); ———, in *Studies in Personality*, O. McNamee and M. A. Merrill, Eds. (McGraw-Hill, New York, 1942), chap. 10.
12. P. Schilder, *Mind, Perception and Thought in Their Constructive Aspects* (Columbia Univ. Press, New York, 1942).
- 27 July 1962

## New High-Pressure Polymorph of Zinc Oxide

**Abstract.** Zinc oxide exists in a sodium chloride structure form in the 100-kilobar pressure range. The cell edge of the high-pressure form is 4.280 Å, the theoretical density is 6.912, and the enthalpy of transition is 785 cal/mole.

Zinc oxide (zincite) has a slightly distorted hexagonal wurtzite structure, and Bragg and Darbyshire (1) have claimed, after electron diffraction of thin films, that it can also exist in a cubic modification with the sphalerite structure. From a qualitative consideration of the effects of high pressures on ionic radii, zinc oxide, if subjected to high pressures, should invert to a NaCl structure. This polymorphic transition

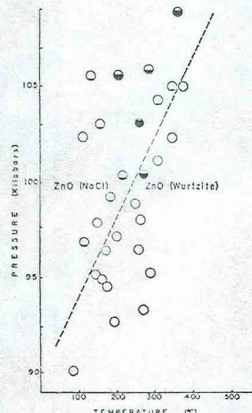


Fig. 1. Plot showing the  $P$ - $T$  conditions for the formation of the NaCl form of ZnO. The dotted line is the approximate equilibrium curve.

21 SEPTEMBER 1962

would produce a primary change in coordination number from four in the wurtzite structure to six in the NaCl structure.

We have synthesized a high-pressure polymorph of zinc oxide with the cubic NaCl structure.

The apparatus used and its accuracy, reproducibility, and limitations are essentially those described by Dachille and Roy (2), who used Bridgman (3) compound anvils. A Rene alloy anvil with a conical insert of grade 886 carbonyl with 3/16-inch effective surface diameter was used for most of the runs. A small drop of saturated ammonium chloride solution was placed on the sample as a catalyst before the pelleted sample was covered with platinum-10-percent rhodium disks and placed between the anvils. The variation in recorded pressure during a single run was not more than  $\pm 6.5$  kbar, as indicated on the Foxboro pressure controller.

In several runs above about 100 kbar a new form of ZnO appeared, and a univariant equilibrium curve between the two polymorphs based on such runs is presented in Fig. 1.

The new phase is identified and characterized by its x-ray powder pattern, which contains the distinctive reflections shown in Table I. No higher angle peaks could be detected in a diffractometer pattern. The  $a_c$  for the NaCl structure phase is 4.280 Å, which gives a theoretical density of 6.912, whereas the density for the zincite structure is 5.680. Conversion could be effected only with ammonium chloride as a catalyst. Other substances, including distilled water and 0.1N sodium carbonate solution, produced no detectable conversion even at pressures well above the equilibrium curve. It would appear that the catalytic action of the ammonium chloride comes from formation of zinc-ammonia complexes. The rate of conversion appears to be very slow and usually a period of 36 to 48 hours is required to produce an appreciable amount of the new phase. Even with long runs the yield is only 30 percent. So far the new phase has not been prepared free from contamination by zincite.

The effect of shear on the phase transition was also studied, by the technique described by Dachille and Roy (4), but no conversion could be detected. However, with shear under pressures of about 100 kbar only short runs without catalyst could be made.

Table I. Distinctive reflections in x-ray powder pattern of new zinc oxide phase.

$hkl$	$d$ (Å)	$I/L$
111	2.479	60
200	2.140	100
222	1.5135	40

Sample extrusion and anvil failure under the high stresses produced were the controlling factors.

The high-pressure polymorph showed no tendency to revert to the wurtzite form even after it had stood for several weeks at room temperature. However, the high-pressure form does revert to the wurtzite structure at as low as 120°C (in 3 weeks). This may suggest that the inability to obtain the NaCl-phase pure may be due to failure of quenching.

The value of  $dp/dT$  as obtained from the equilibrium curve gives a value of 42.5 atm/°C, yielding a  $\Delta H$  of transition from the Clapeyron relation of 785 cal/mole at 25°C (5).

CARL H. BATES  
WILLIAM B. WHITE  
RUSTUM ROY

Materials Research Laboratory,  
Pennsylvania State University,  
University Park

### References and Notes

- W. L. Bragg and J. A. Darbyshire, *Trans. Faraday Soc.* 28, 522 (1932).
- F. Dachille and R. Roy, *Modern Very High Pressure Techniques* (Butterworths, London, 1962), chap. 9, pp. 163-180.
- P. W. Bridgman and I. Simon, *J. Appl. Phys.* 24, 405 (1953).
- F. Dachille and R. Roy, in *Reactivity of Solids*, J. H. De Boer, Ed. (Elsevier, Amsterdam, 1961), pp. 502-511.
- This work was supported by the American Zinc Institute through a fellowship held by one of us (C.H.B.). This report is contribution No. 62-13 of the College of Mineral Industries, Pennsylvania State University.

2 August 1962

## A Gene in *Drosophila* That Produces a New Chromosomal Banding Pattern

**Abstract.** A change in the banding pattern of the distal end of the third chromosome in *Drosophila pseudoobscura* has been found. It appears to be produced by homozygosis for a recessive gene, which is called "salivary" (*sal*) in this report.

In the course of an experiment dealing with inversion polymorphism in *Drosophila pseudoobscura* (1), a new banding pattern, at the distal end of the third chromosome, was observed by one of us (L.L.) (Fig. 1). It was

993

Bates, White, and Roy, **Science**, 137, 993 (1962)

Wurtzite (B4) to NaCl (B1) around 9 GPa

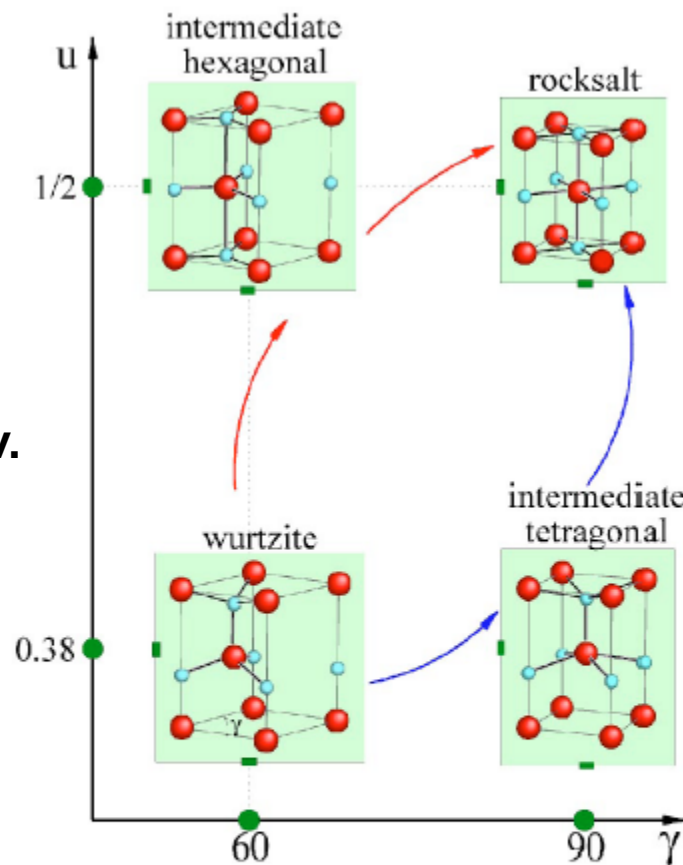
Ammonium chloride solution as a catalyst.

## Mechanism of B4-to-B1 Transition: Path

S. Limpijumnong, and S. Jungthawan, **Phys. Rev. B**, 70, 054104 (Aug. 2004).

S. Limpijumnong, and W. R. L. Lambrecht, **Phys. Rev. Lett.**, 86, 91 (2001).

L. Bellaiche, K. Kunc, and J. M. Besson, **Phys. Rev. B**, 54, 8945 (1996)



A. M. Saitta, and F. Decremps, **Phys. Rev. B**, 70, 035214 (July, 2004)

FIG. 1. (Color online) The four structures in the  $ab$  angle- $u$  internal coordinate plane. The optimal  $c/a$  ratio is about 1.61 and 1.74 for the wurtzite and tetragonal structures (bottom), where  $u \approx 0.38$ , and 1.29 and  $\sqrt{2}$  for the hexagonal and rocksalt structures (top), where  $u=1/2$ .

## Diffraction studies at ambient and HP conditions

B4 phase Zn-O: 1.992 Å and 1.973 Å

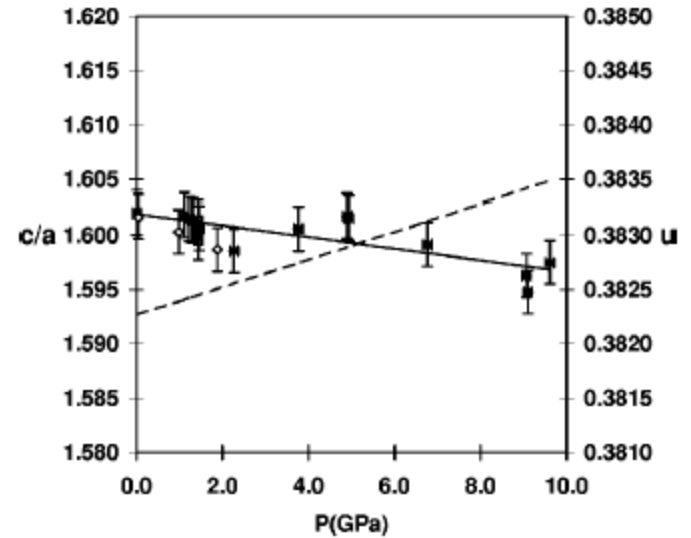
S. C. Abrahams, and J. L. Bernstein, **Acta Cryst. B** 25, 1233, (1969).

The ideal correlation:

$$u(c/a) = (3/8)^{1/2} \quad (u = 3/8; c/a = (8/3)^{1/2})$$

between  $c/a$  ratio and  $u$ , which was experimentally confirmed by the wurtzite structural refinements of ZnO and ZnS at ambient conditions.

E. H. Kisi, and M. M. Elcombe, **Acta Cryst. C** 45, 1867, (1989).



S. Desgreniers, **Phys. Rev. B**, 58, 14102 (1998).

“Obvious questions which arise are whether the ideal correlation are affected by the compression”

# High resolution ADXRD high pressure experiment in HPCAT

Polycrystalline ZnO (99.9995%);

Helium pressure medium;

Ruby ball pressure marker;

Monitored until close equilibrium at each pressure change;

Average pressure before & after measurement;

Room temperature;

Thickness at 1 bar:

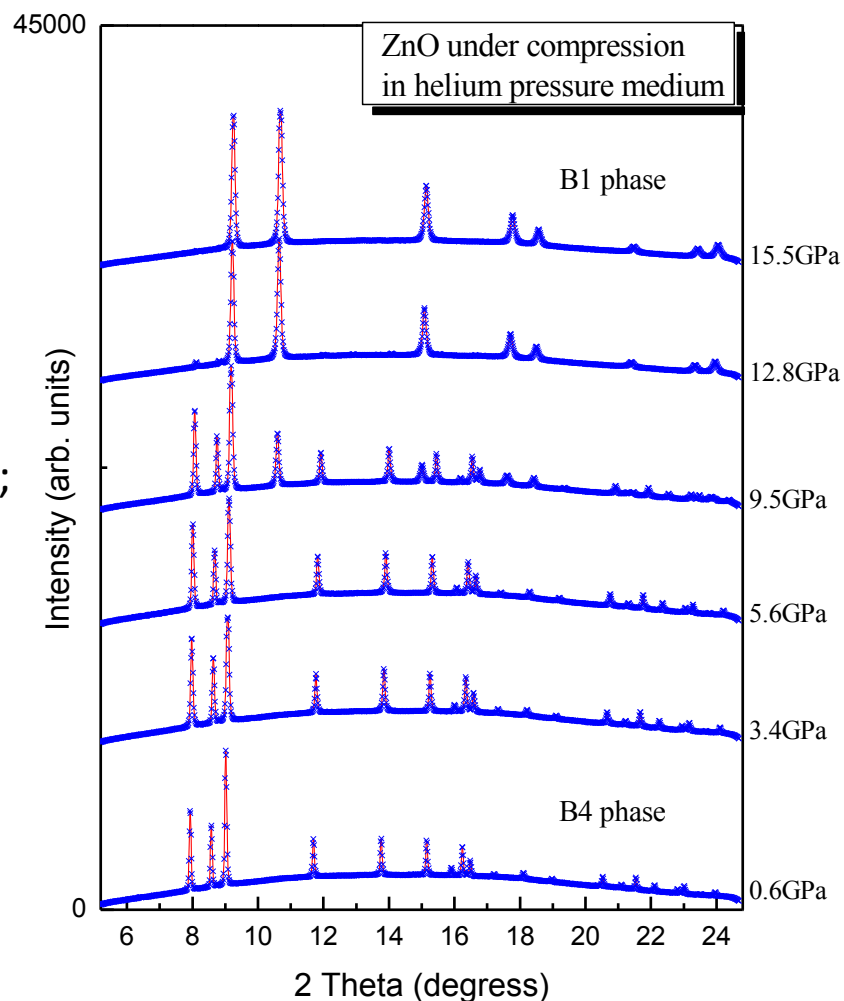
Sample:  $\sim 5 \mu\text{m}$

T301 Gasket:  $\sim 45 \mu\text{m}$

$\lambda = 0.3888 \text{ \AA}$ ;

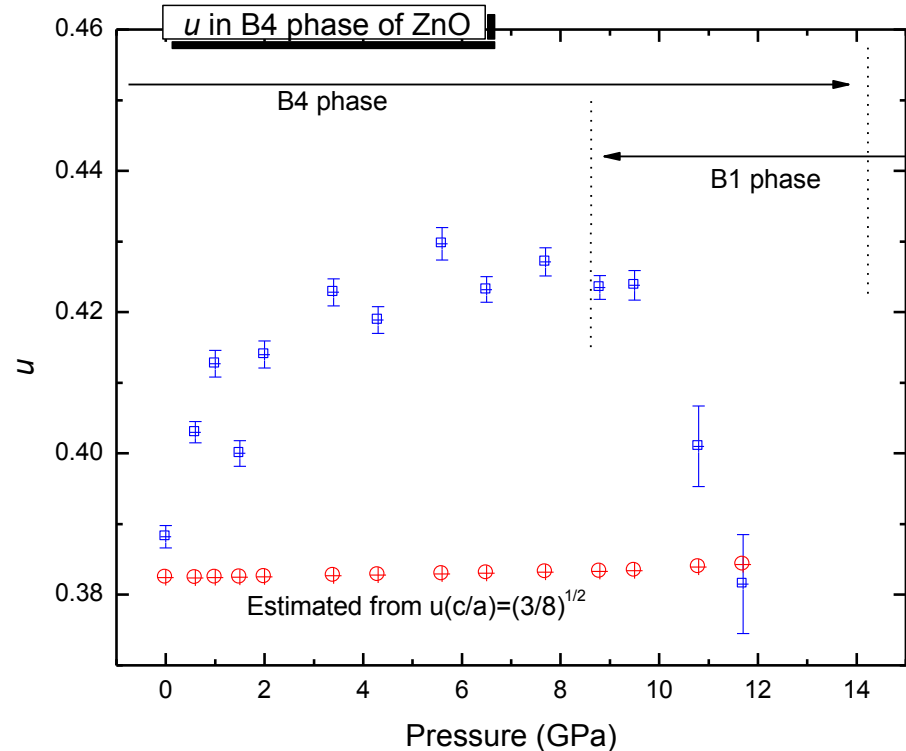
Beam size:  $\sim 15 \mu\text{m}$ ;

MAR345 IP



# The $u$ and the Transition Path

- In spite of the  $c/a$  ratio shows a slight decrease with pressure, the  $u(P)$  trend in our experimental results show that the initial intermediate distortion path prefers the ‘hexagonal’ model than the ‘tetragonal’ model up to 5.6 GPa.
- The ‘hexagonal’ intermediate path is not the ideal one used in calculations. Therefore, any change of the  $c/a$  ratio would counter the variation of  $u$  under pressure.
- The  $u$  values quickly decrease during phase transition pressure range may imply that this distortion ‘hexagonal’ intermediate phase is in competition with the alternative path.



Pre-transitional effect:

initial intermediate distortion path

Haozhe Liu, Yang Ding, Maddury Somayazulu, et al., Rietveld refinement study of the pressure dependence of internal structural parameter  $u$  in wurtzite phase of zinc oxide, **Physical Review B**, 71, 212103, 2005.

# Why ultra-high pressure?

Total energy and  
electronic structure  
calculations

B1 (NaCl) to B2 (CsCl)  
transition at:

260 GPa (LDA)

256 GPa (GGA)

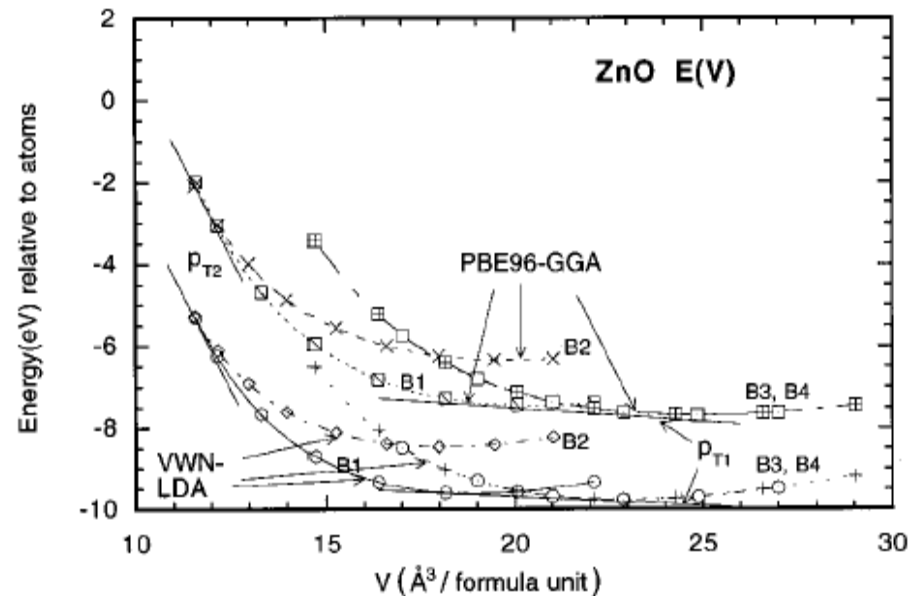
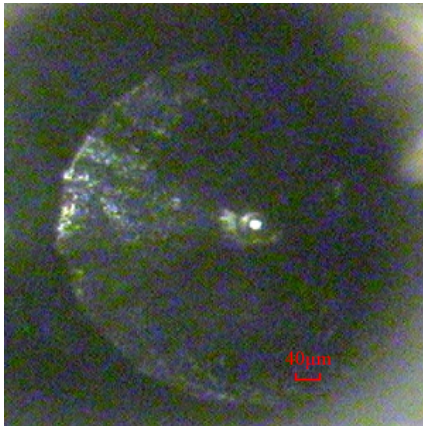


FIG. 1. Energy versus volume per formula unit for ZnO in the B4, B3, B1, and B2 structures, showing the common tangent construction for transition pressures.

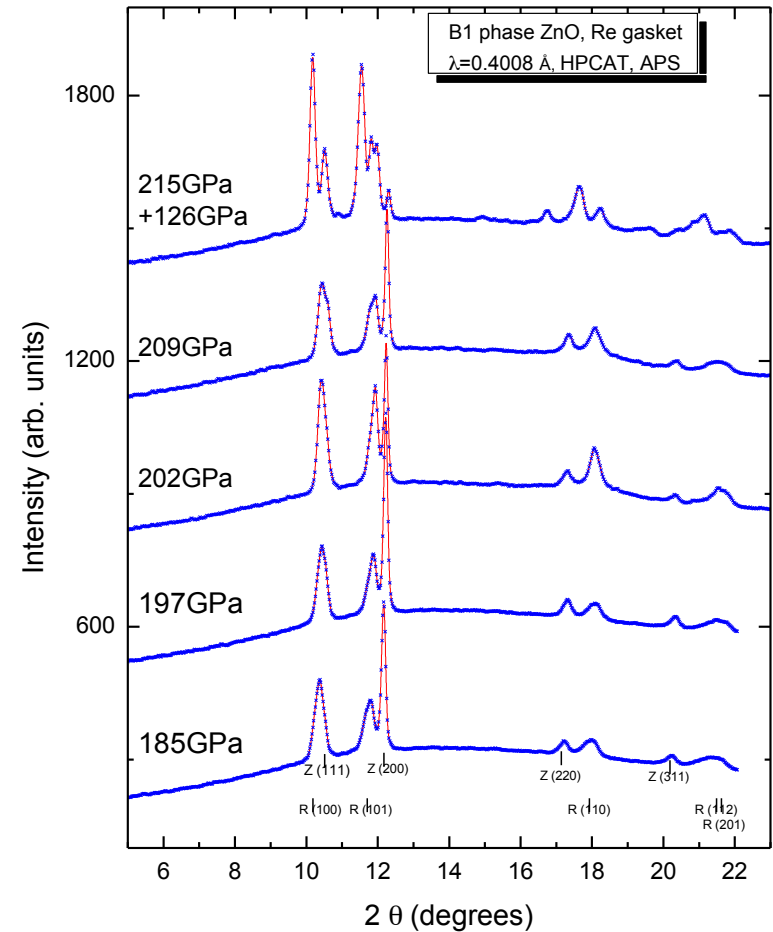
J. E. Jaffe, J. A. Snyder, Z. Lin, and A. C. Hess, **Phys. Rev. B**, 62, 1660 (2000).

# High Pressure ADXRD at HPCAT

ZnO as pressure marker;  
No pressure medium;  
Rhenium gasket;  
IP or CCD (30 s).

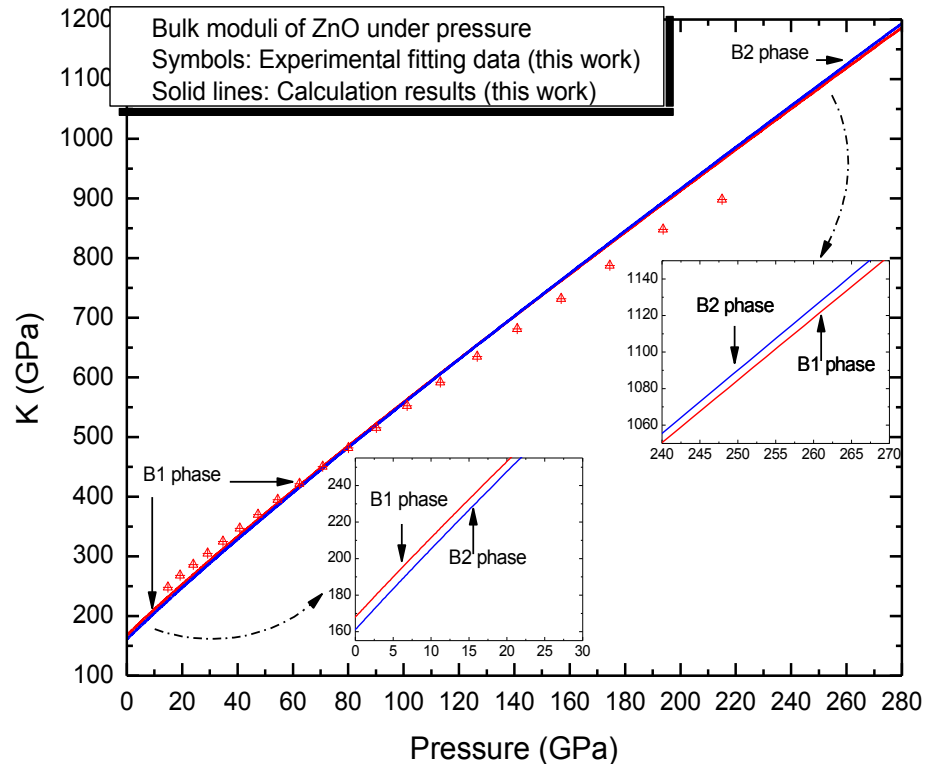
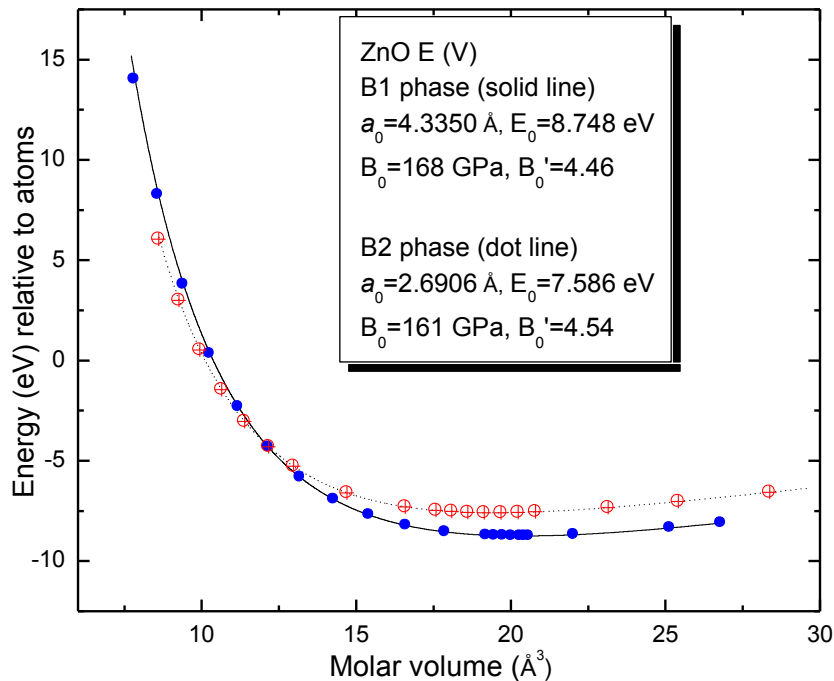


~132 GPa (12/11/2004)



Reliability of the predictions?

# Total energy calculations for the B1 and B2 phase of ZnO



Equilibrium transition pressure was estimated at about 261 GPa, **Need Run #4!**

Haozhe Liu, John S. Tse, and Ho-kwang Mao, Stability of rocksalt phase of zinc oxide under strong compression: Synchrotron x-ray diffraction experiments and first-principles calculations studies, **Journal of Applied Physics**, 2006.

## Next Door Neighbor: CdO

- the  $3d$  and  $4d$  transition-metal monoxide ZnO and CdO
- Cd: end member of the transition metal group,  $[\text{Kr}].4d^{10}.5s^2$ , similar to IIA main group elements

The first principles DFT total energy calculations:

rock-salt (B1), cesium chloride (B2), nickel arsenide, zinc-blende, orthorhombic cmcm, cinnabar, and wurtzite structures

Prediction: B1 to B2 transition  $\sim 89\text{GPa}$ .

(common behavior in alkali and ammonium halides, some IIA-VIA compounds under pressure)

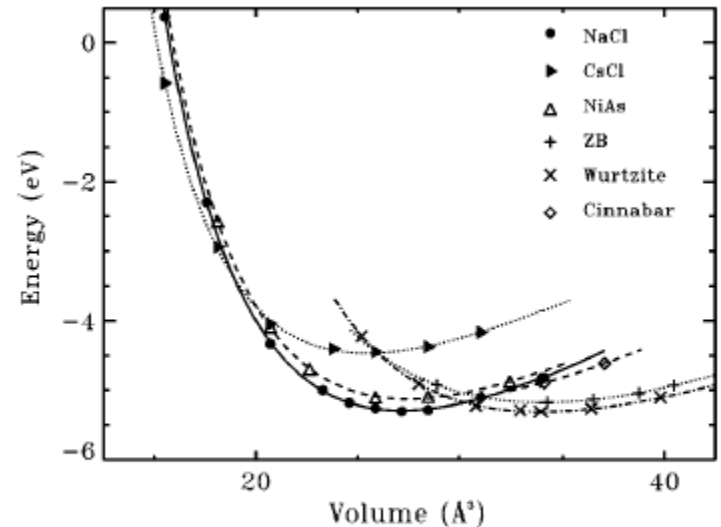
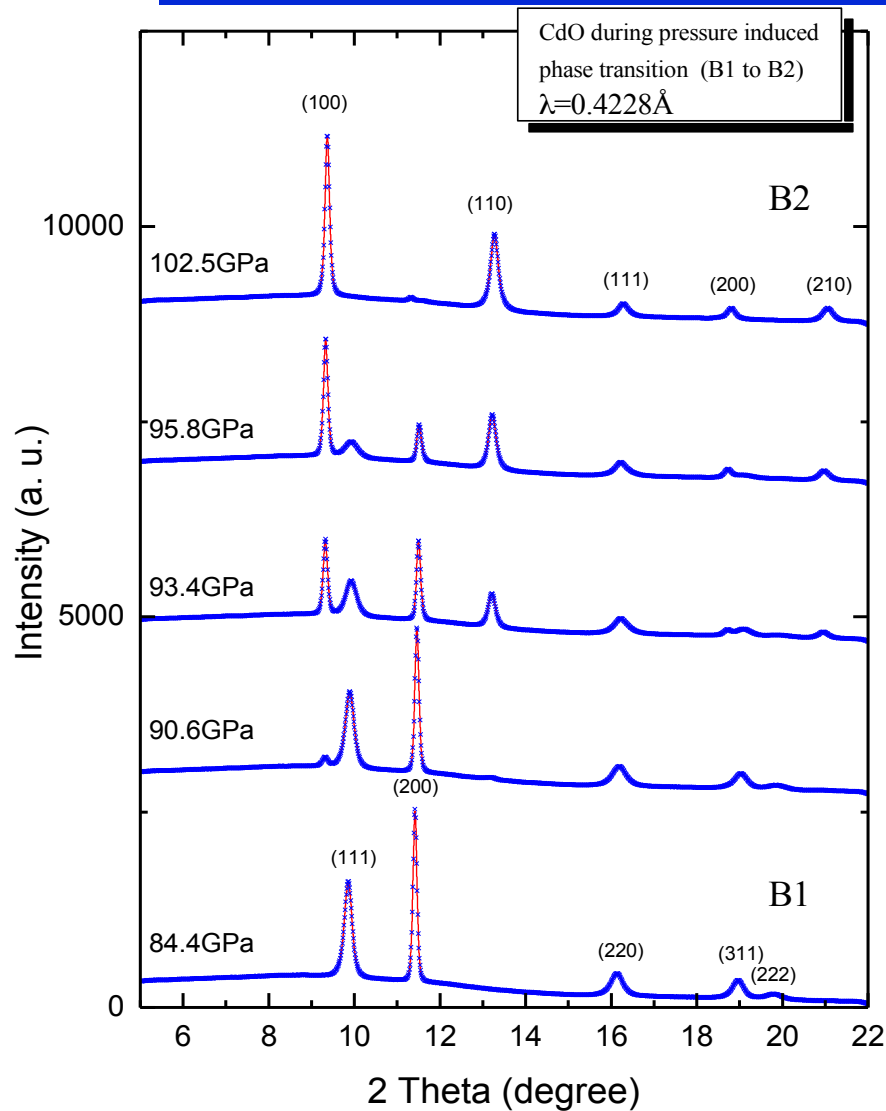


FIG. 2. Total energy (in eV per formula unit) versus the atomic volume (in  $\text{\AA}^3$ ) for several structures of CdO.

R. J. Guerrero-Moreno, N. Takeuchi, **Phys. Rev. B** 66, 205205 (2002).

# High Pressure ADXRD for CdO at HPCAT



Run #2 (Feb. 2004):

Polycrystalline CdO (99.998%);

No pressure medium;

Au pressure marker;

Room temperature;

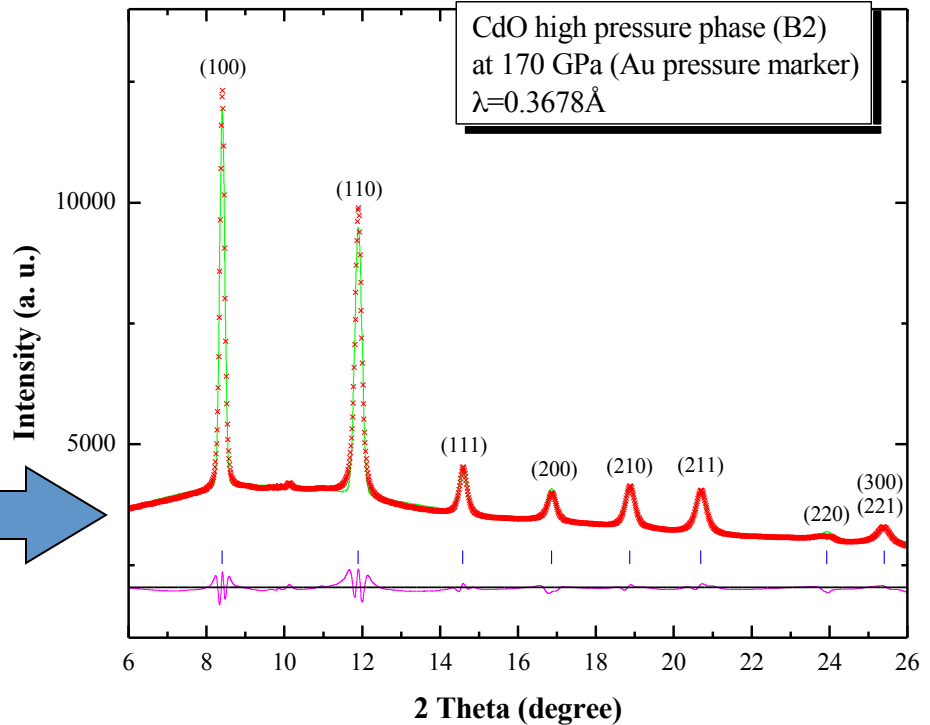
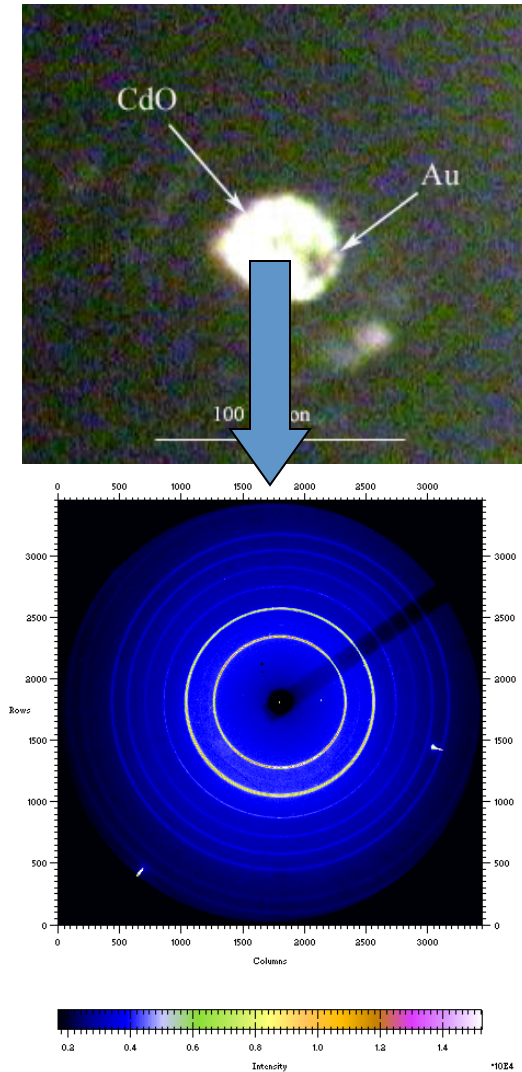
Rhenium gasket;

Beam size:  $\sim 10\ \mu\text{m}$ ;

MAR345 IP

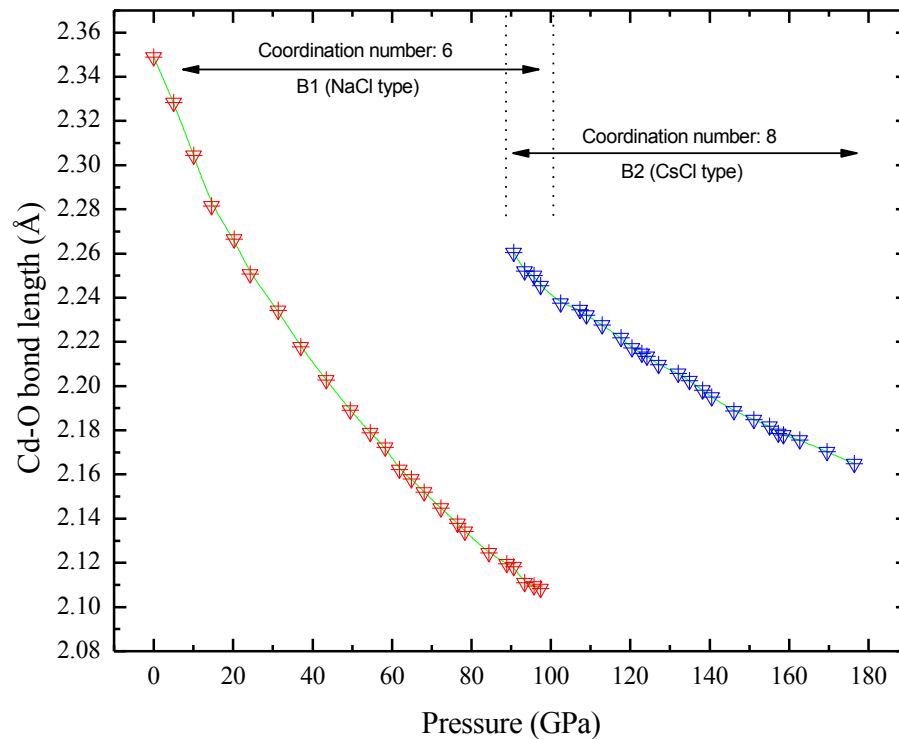
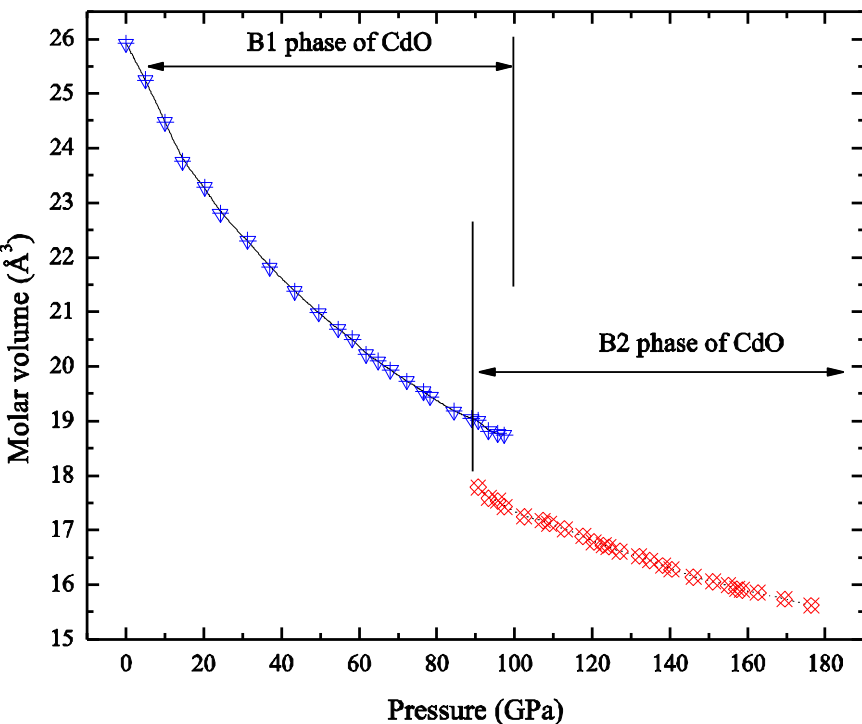
# High Pressure ADXRD for CdO at HPCAT

~170 GPa

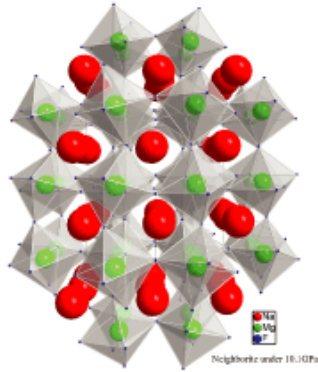


Haozhe Liu, Ho-kwang Mao, Maddury Somayazulu, et al., B1-to-B2 phase transition of transition-metal monoxide CdO under strong compression, **Physical Review B**, 70, 094114, 2004.

# High Pressure ADXRD for CdO at HPCAT

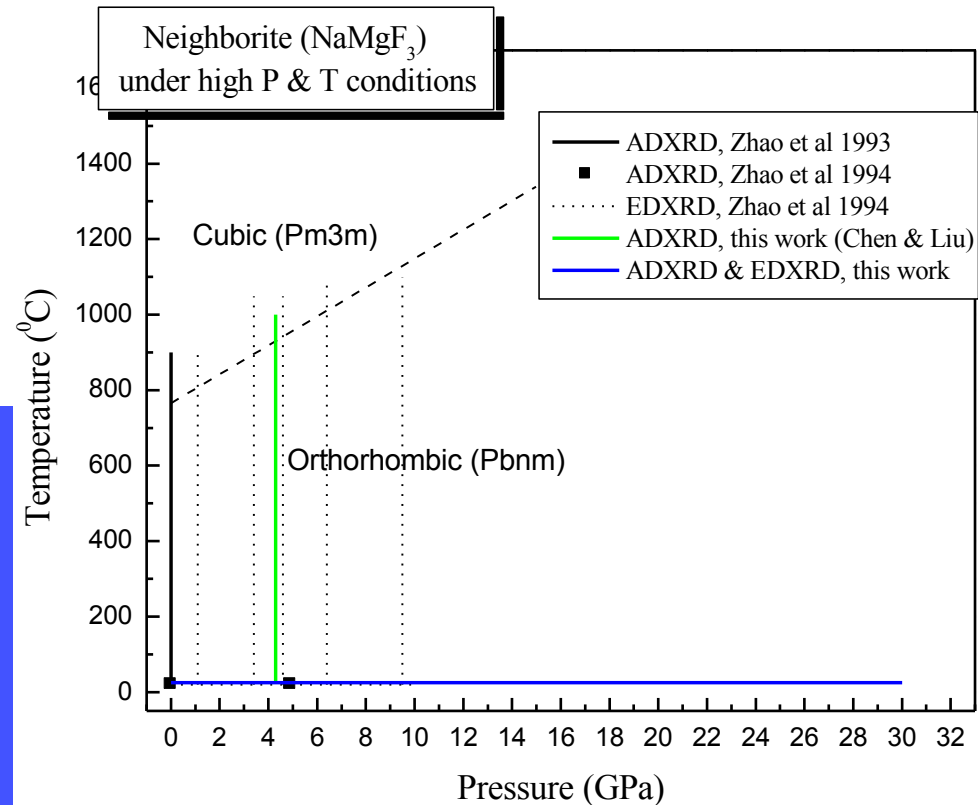


**First case** for the B1-to-B2 directly phase transition in d transition-metal monoxides under pressure.



High-pressure tests on materials found in lower mantle • Overstrating spin  
hydrous in northern Gulf of Mexico • Spikes caused by intradial electricity?

## Neighborite: $\text{NaMgF}_3$



Jiuhua Chen, Haozhe Liu, C. David Martin, et al., Crystal chemistry of  $\text{NaMgF}_3$  perovskite at high pressure and temperature, *American Mineralogist*, 90(10), 1534-1539, 2005.

An ideal **analogue** model for silicate perovskite ( $\text{MgSiO}_3$ ) due to the similarities between their crystal and electronic structures.

**Advantage:** weaker bonding feature of neighborite grant us the opportunity to simulate behavior of silicate perovskite at lower mantle, i. e. high pressure and high temperature condition, at relatively lower P-T conditions.

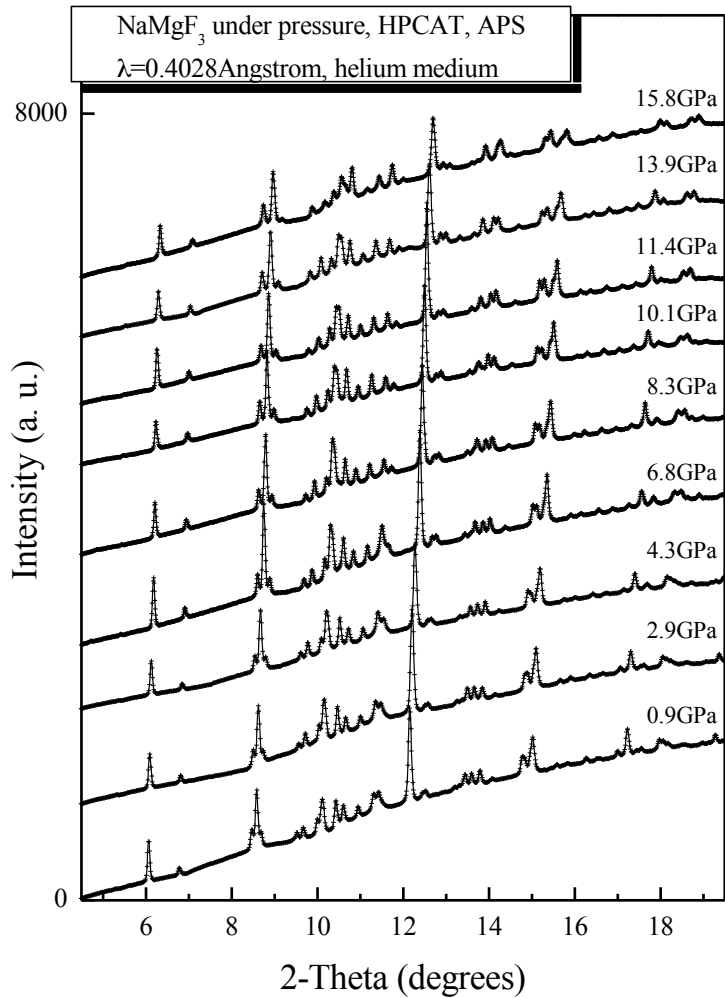
Okeeffe M, Bovin JO, Solid electrolyte behavior of  $\text{NaMgF}_3$ : geophysical implications, *Science*, 206 (4418): 599-600, 1979.

## Neighborite under high pressure at RT



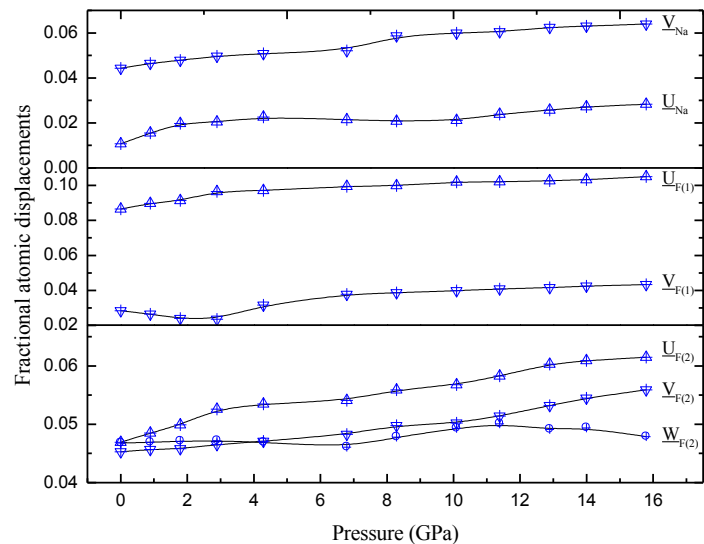
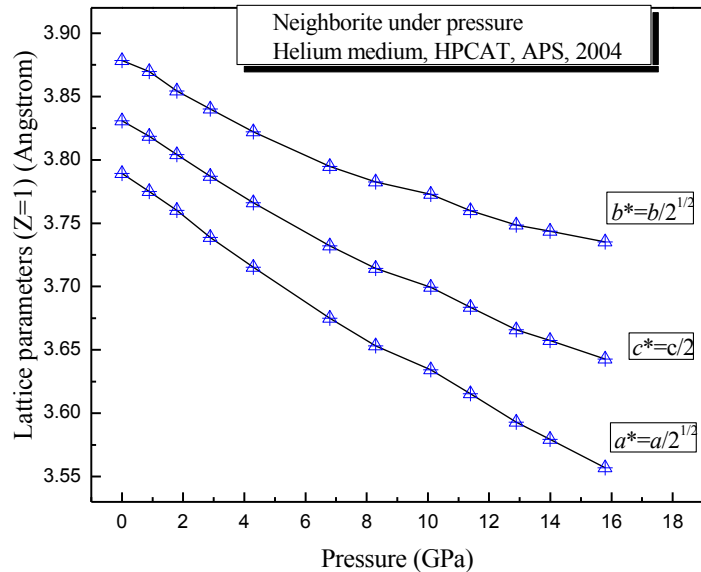
*In situ* high pressure XRD DAC experiments:

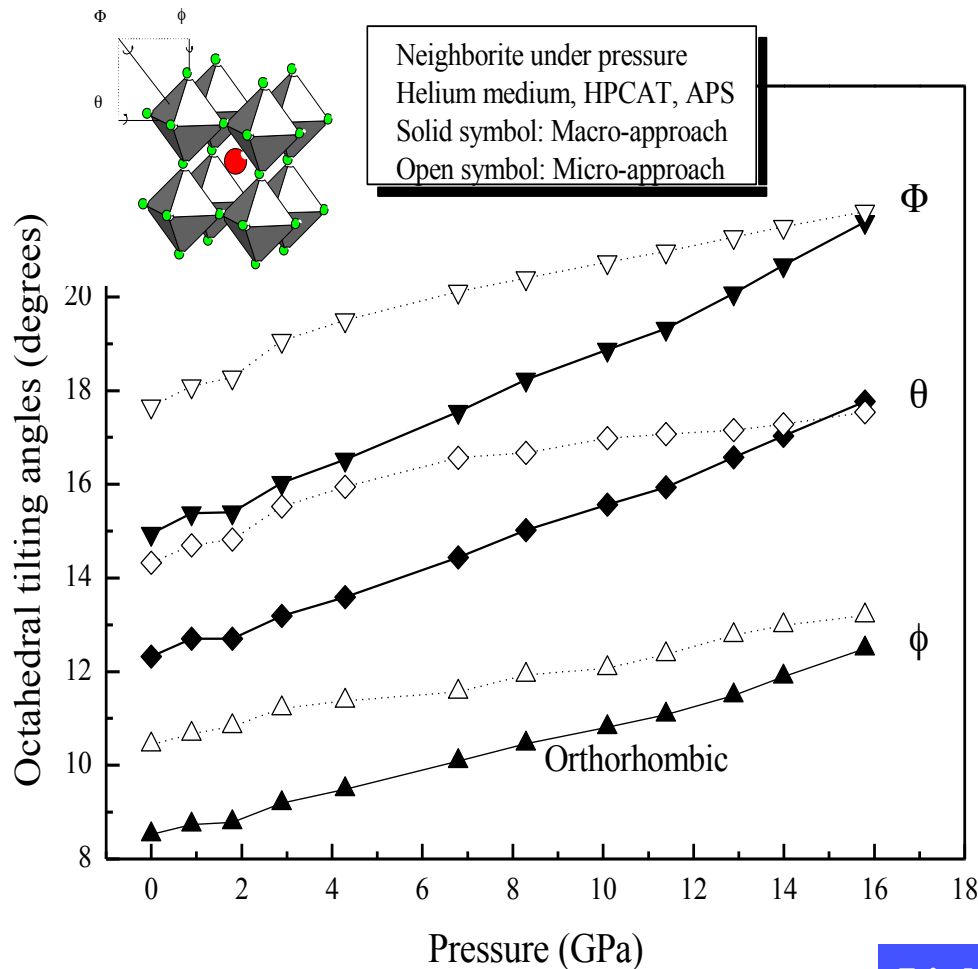
1. EDXRD, Silicone oil, 22 GPa, X17C, NSLS, 2/4-9/03
2. ADXRD, Silicone oil, 22 GPa, HPCAT, APS, 2/18-22/03
3. EDXRD, Methanol/ethanol, 30 GPa, X17C, NSLS, 3/6-9/03
4. ADXRD, Silicone oil, 30 GPa, X17C, NSLS, 4/10-13/03
5. ADXRD, Silicone oil, 53 GPa, X17C, NSLS, 9/21-22/03
6. ADXRD, Helium, 16 GPa, HPCAT, APS, 2/7-8/04



Fractional atomic coordinates for *Pbnm*

	x	y	z
Na	$1-U_{Na}$	$V_{Na}$	0.25
Mg	0	0.5	0
F(1)	$U_{F(+)}$	$0.5-V_{F(+)}$	0.25
F(2)	$0.75-U_{F(2)}$	$0.25+V_{F(2)}$	$W_{F(2)}$





**Macro-derived tilting  
(from lattice parameters)**

$\cos\theta = a/b$   
 $\cos\phi = 2^{1/2}a/c$   
 $\cos\Phi = \cos\theta\cos\phi$

**Micro-derived tilting:  
(from atomic displacements)**

$\tan\theta = 4(u_{F(1)}^2 + v_{F(1)}^2)^{1/2}/c = 32^{1/2}w_{F(2)} / (a^2 + b^2)^{1/2}$   
 $\tan\phi = 4(u_{F(2)}^2 + v_{F(2)}^2)^{1/2}/(a^2 + b^2)^{1/2}$   
 $\cos\Phi = \cos\theta\cos\phi$

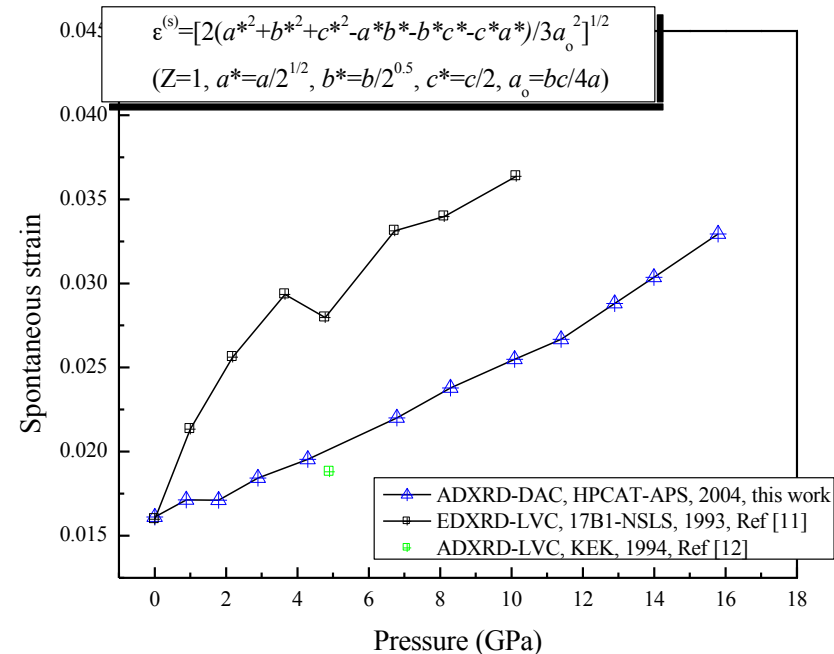
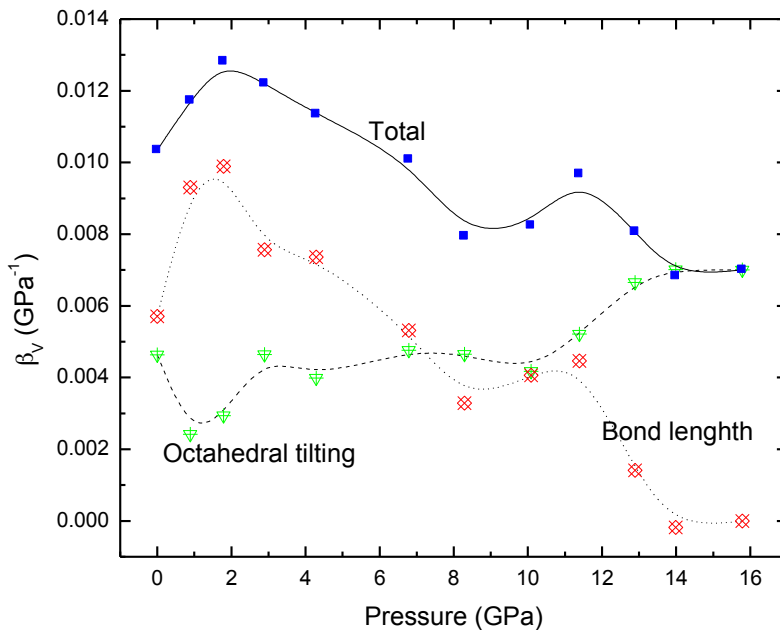
**Link between micro- and macro approach for tilting**

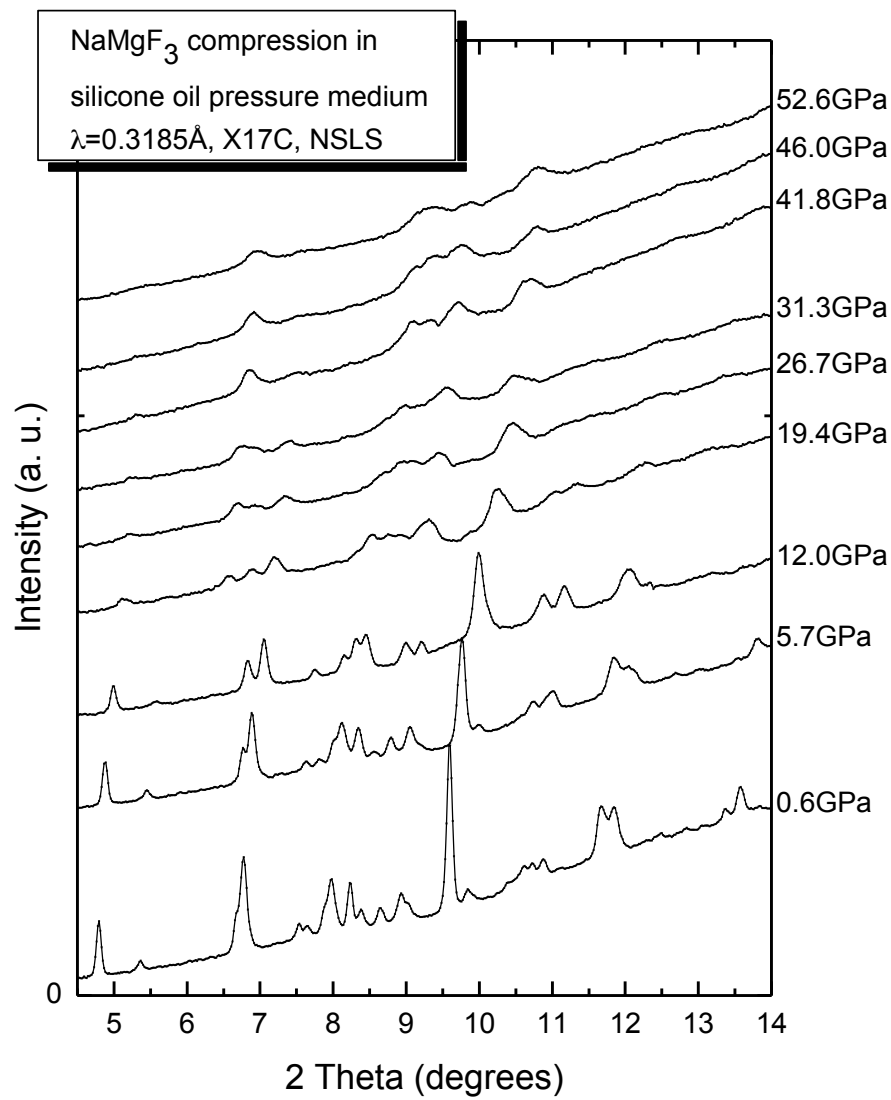
$\Phi_{xyz} = 1.19\Phi_{abc} - 0.174$       0~7GPa, T=25°C  
 $\Phi_{xyz} = 0.428\Phi_{abc} + 12.6$       7~16GPa, T=25°C

# Contribution of octahedral tilting and the octahedral bond length to the volumetric compression:

## Spontaneous strain

$$\beta_V = \beta_{V_0} + \beta_{V_\Phi} = \frac{-3\partial[Mg - F]}{[Mg - F]\partial P} + \frac{-2\partial \cos\Phi}{\cos\Phi\partial P}$$





HP phase could be indexed with the layering-type **post-perovskite** structural model with space group *Cmcm*.

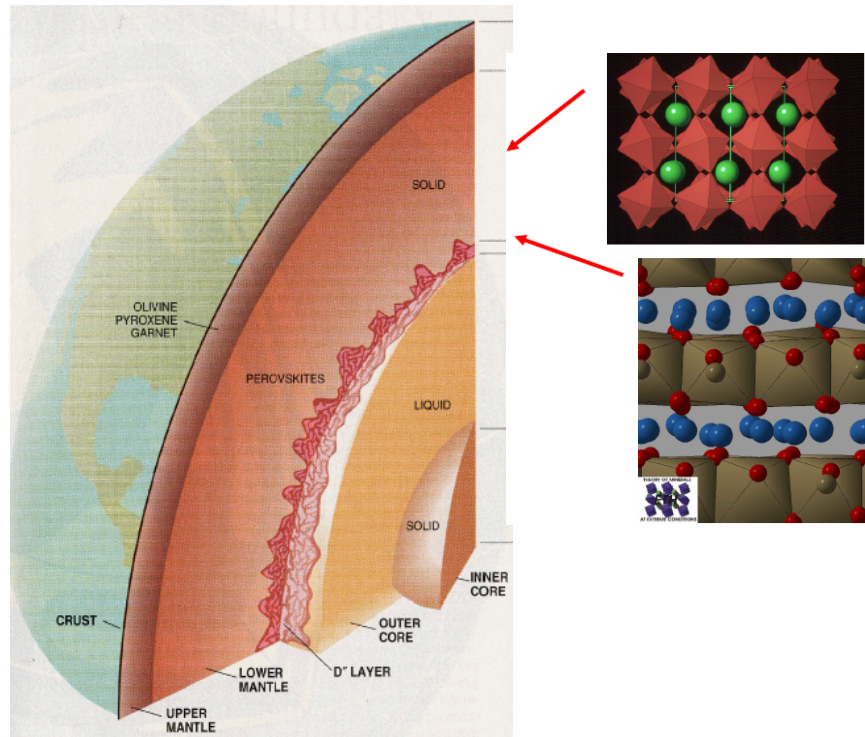
$a=2.780\text{ \AA}$ ,  $b=8.491\text{ \AA}$ , and  $c=7.001\text{ \AA}$  at 31.3GPa

Analog: for silicate perovskite ( $\text{MgSiO}_3$ ) to post-perovskite transition at high pressure and high temperature (lowermost mantle, D'' layer) conditions.

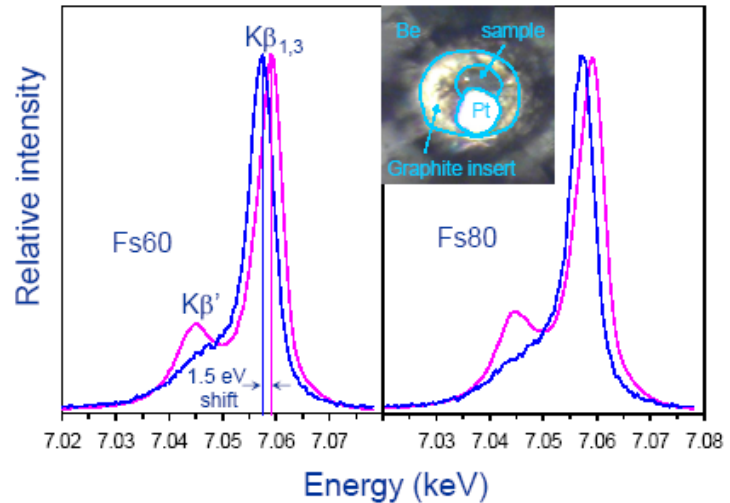
Two independent theoretical calculations [Parise et al., 2004; Oganov, 2005] confirmed this pressure induced phase transition.

Further studies: Dave Martin et al.

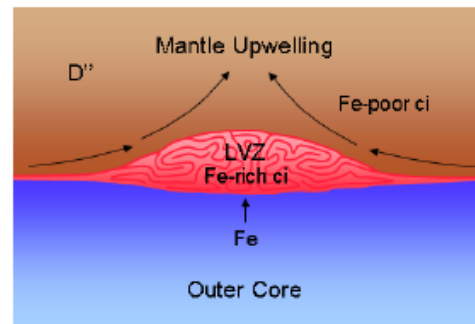
# New phases at the core mantle boundary: Electronic and elastic properties of (Mg, Fe)SiO<sub>3</sub> post-perovskite



## X-ray Emission



• (Mg,Fe)SiO<sub>3</sub> post-perovskite is low spin



Mao et al, *Science*, 312, 564, 2006



*Robert Boyle*

## EFFECTS OF PRESSURE ON GASES

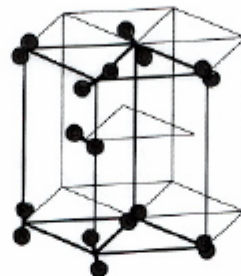
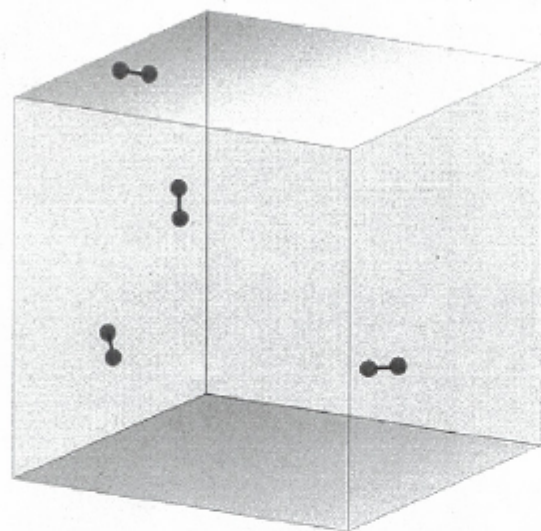
**Gas Laws:**

$$\text{Pressure} \times \text{Volume} = \text{Constant}$$

**... perhaps the pressure of the air might have an interest in more phaenomena than men have hitherto thought.”**

*Touching the Spring of the Air,*

*New Experiments in Physics and Mechanics, XLIII 1660*

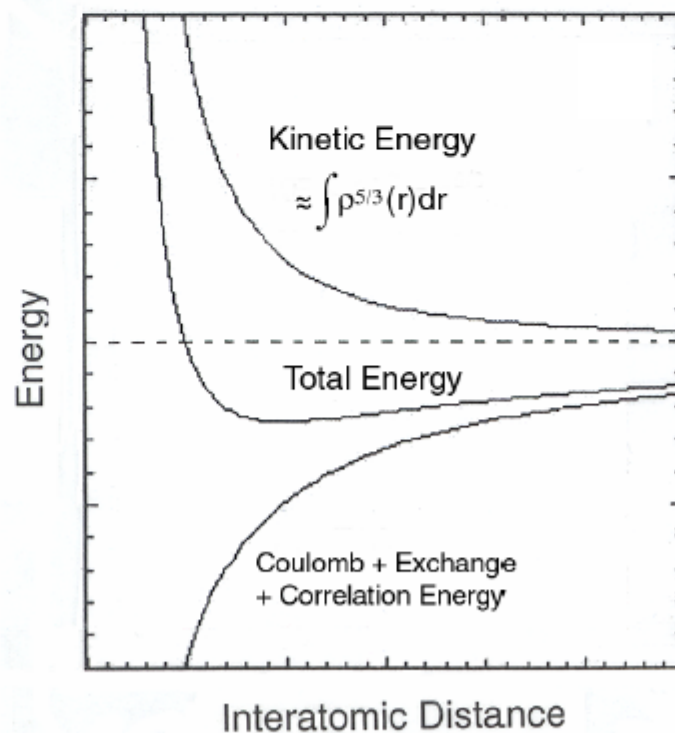


$$P = - \frac{\partial E}{\partial V}$$

## ENERGY AND INTERPARTICLE DISTANCES

*atomic*  
*molecular*  
*nuclear*

*electronic*  
*nanoparticle*  
*intercellular...*



# Hydrogen occupies a unique position in the Periodic Table

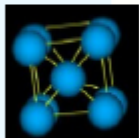
## 1. 'SIMPLE' MOLECULES



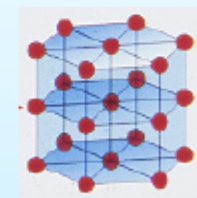
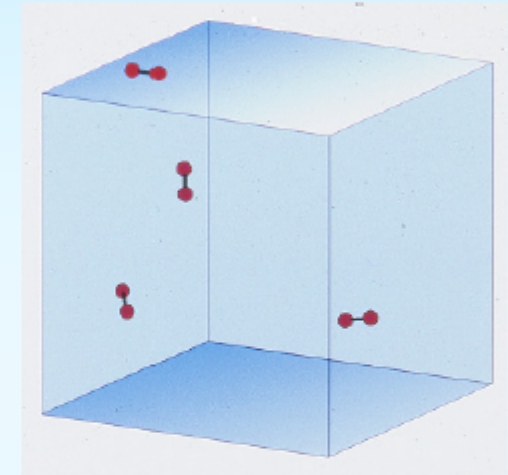
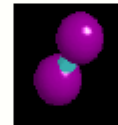
Alkalis

Halogens

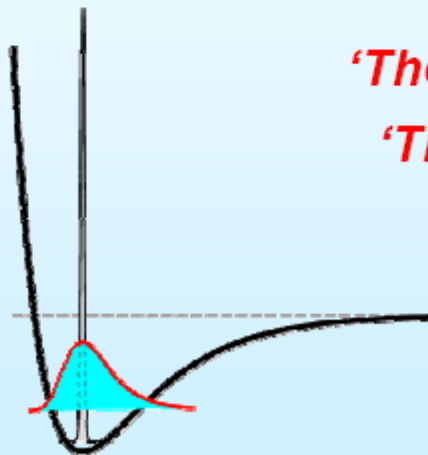
1 H	← ? →																1 H	2 He
3 Li	4 Be											5 B	6 C	7 N	8 O	9 F	10 Ne	
11 Na	12 Mg											13 Al	14 Si	15 P	16 S	17 Cl	18 Ar	
19 K	20 Ca	21 Sc	22 Ti	23 V	24 Cr	25 Mn	26 Fe	27 Co	28 Ni	29 Cu	30 Zn	31 Ga	32 Ge	33 As	34 Se	35 Br	36 Kr	
37 Rb	38 Sr	39 Y	40 Zr	41 Nb	42 Mo	43 Tc	44 Ru	45 Rh	46 Pd	47 Ag	48 Cd	49 In	50 Sn	51 Sb	52 Te	53 I	54 Xe	
55 Cs	56 Ba	57 La	72 Hf	73 Ta	74 W	75 Re	76 Os	77 Ir	78 Pt	79 Au	80 Hg	81 Tl	82 Pb	83 Bi	84 Po	85 At	86 Rn	
87 Fr	88 Ra	89 Ac	104 Ru	105 Ha	106 Unh	107 Uns	108 Uno	109 Une	110 Unf									



58 Ce	59 Pr	60 Nd	61 Pm	62 Sm	63 Eu	64 Gd	65 Tb	66 Dy	67 Ho	68 Er	69 Tm	70 Yb	71 Lu
90 Th	91 Pa	92 U	93 Np	94 Pu	95 Am	96 Cm	97 Bk	98 Cf	99 Es	100 Fm	101 Md	102 No	103 Lr

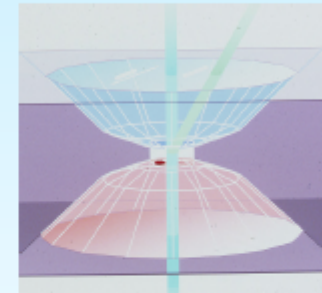
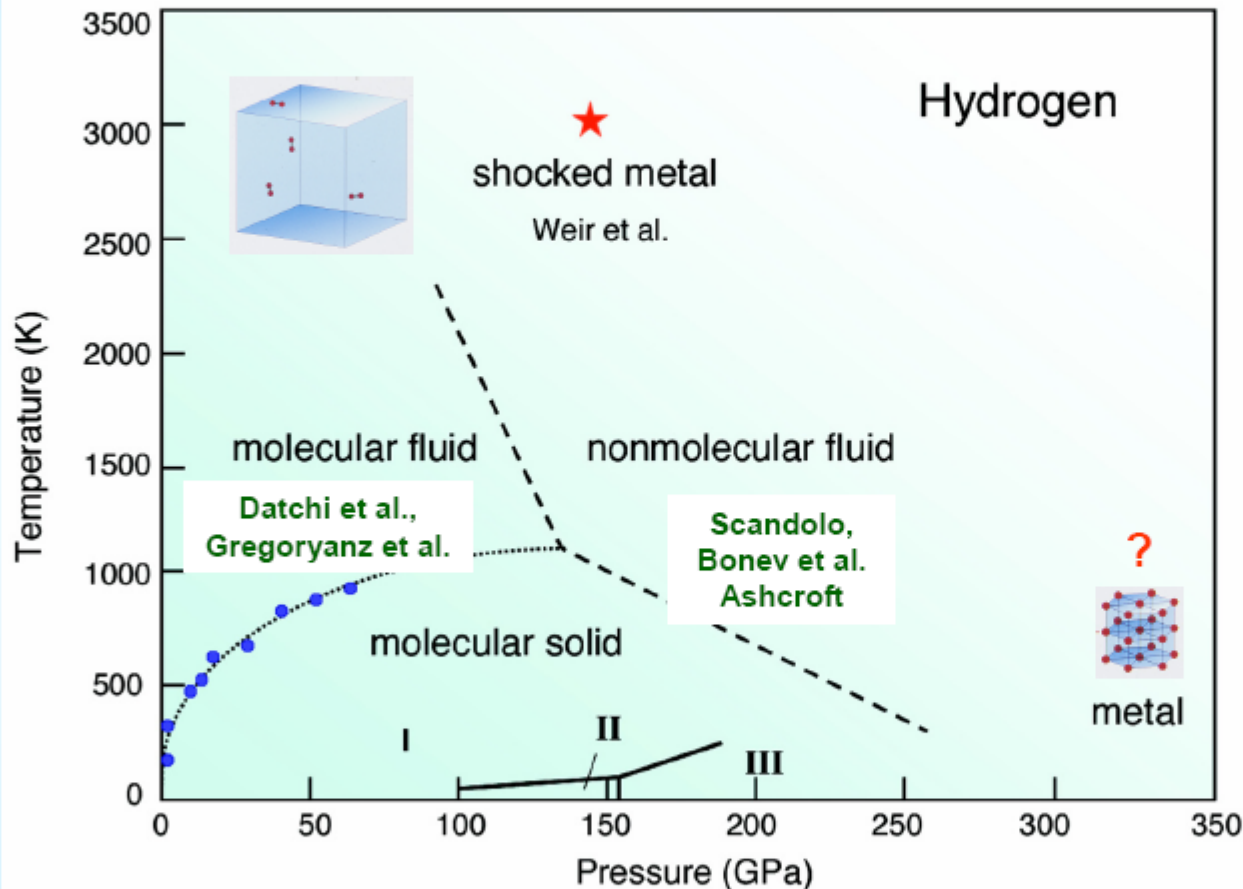


*'The Element of Uncertainty'*  
*'The Element of Surprise'*

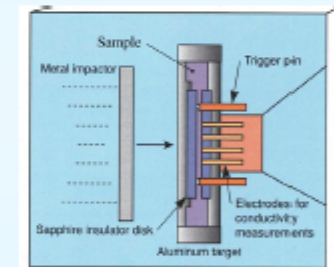


**A metal (>25 GPa)?**  
[Wigner & Huntington, (1935)]

# Unexpected phase diagram of hydrogen



STATIC



DYNAMIC



THEORY

- MOLECULES STABLE TO ~300 GPa (<300 K)
- HIGH P-T DISSOCIATION PREDICTED
- HIGH- $T_c$  SUPERCONDUCTOR AND SUPERFLUID?

# Periodic Table of the Elements

**PRESSURE**

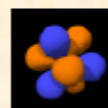


**PRESSURE**

→

1 1A 1 H 1.008	2 Alkaline earth metals 2A 4 Be 9.012											13 3A 5 B 10.81	14 4A 6 C 12.01	15 5A 7 N 14.01	16 6A 8 O 16.00	17 Halogens 7A 9 F 19.00	18 Noble gases 8A 2 He 4.003
3 Li 6.941	11 Na 22.99	3	4	5	6	7	8	9	10	11	12	13 Al 26.98	14 Si 28.09	15 P 30.97	16 S 32.07	17 Cl 35.45	18 Ar 39.95
19 K 39.10	20 Ca 40.08	21 Sc 44.96	22 Ti 47.88	23 V 50.94	24 Cr 52.00	25 Mn 54.94	26 Fe 55.85	27 Co 58.93	28 Ni 58.69	29 Cu 63.55	30 Zn 65.38	31 Ga 69.72	32 Ge 72.59	33 As 74.92	34 Se 78.96	35 Br 79.90	36 Kr 83.80
37 Rb 85.47	38 Sr 87.62	39 Y 88.91	40 Zr 91.22	41 Nb 92.91	42 Mo 95.94	43 Tc (98)	44 Ru 101.1	45 Rh 102.9	46 Pd 106.4	47 Ag 107.9	48 Cd 112.4	49 In 114.8	50 Sn 118.7	51 Sb 121.8	52 Te 127.6	53 I 126.9	54 Xe 131.3
55 Cs 132.9	56 Ba 137.3	57 La* 138.9	72 Hf 178.5	73 Ta 180.9	74 W 183.9	75 Re 186.2	76 Os 190.2	77 Ir 192.2	78 Pt 195.1	79 Au 197.0	80 Hg 200.6	81 Tl 204.4	82 Pb 207.2	83 Bi 209.0	84 Po (209)	85 At (210)	86 Rn (222)
87 Fr (223)	88 Ra 226	89 Ac* (227)	104 Unq	105 Unp	106 Unh	107 Uns	108 Uno	109 Une									

metals ← → nonmetals



*Lanthanides	58 Ce 140.1	59 Pr 140.9	60 Nd 144.2	61 Pm (145)	62 Sm 150.4	63 Eu 152.0	64 Gd 157.3	65 Tb 158.9	66 Dy 162.5	67 Ho 164.9	68 Er 167.3	69 Tm 168.9	70 Yb 173.0	71 Lu 175.0
*Actinides	90 Th 232.0	91 Pa (231)	92 U 238.0	93 Np (237)	94 Pu (244)	95 Am (243)	96 Cm (247)	97 Bk (247)	98 Cf (251)	99 Es (252)	100 Fm (257)	101 Md (258)	102 No (259)	103 Lr (260)

- Filling of *s*, *p*, *d*, ... orbitals
- Simple structures

